공학박사 학위논문

Catalytic Depolymerization of Lignin to Value-added Chemicals in Supercritical Ethanol

초임계 에탄올에서 고부가가치 화합물 생산을 위한 리그닌의 촉매적 분해반응

2017년 8월

서울대학교 대학원

화학생물공학부

정 소 연

Abstract

Catalytic Depolymerization of Lignin to Value-added Chemicals in Supercritical Ethanol

Soyeon Jeong
School of Chemical and Biological Engineering
The Graduate School
Seoul National University

Finding alternative resources is inevitable as the conventional fossil fuels are rapidly depleted due to the increasing demand. In this respect, biomass is the most abundant renewable carbon resources so that it is considered as one of the promising alternative chemicals. Especially, lignocellulosic biomass, the second-generation biomass does not have a 'food vs. fuel' issue like the first-generation biomass. Therefore, the supply of lignocellulosic biomass is relatively easy compared with the other resources. Especially, lignin, one of the constituents of lignocellulosic biomass, is an amorphous co-polymer consisting of various aromatic compounds, cross-linked by C-C and C-O bonds. Therefore, it has considerable potential to be used as value-added chemicals. Meanwhile, the amount of C-O bonds in lignin such as β-O-4 (46 ~ 60 %), α-O-4 (6 ~8 %) and 4-O-5 (3.5 ~ 6.5 %) is much more than that of C-C bonds in lignin such as

β-β (7 %), β-5 (6 ~ 12 %), β-1 (4.5 ~11 %) and 5-5 (2 ~3 %). Hence, the selective cleavage of C-O bonds in lignin is considered as an essential process to depolymerize lignin into value-added chemicals.

For the decades, various thermochemical processes such as pyrolysis, gasification, catalytic cracking and solvolysis have been applied for depolymerization lignin in order to get the high yield of value-added chemicals. However, the recalcitrant structures of lignin make it hard to be converted into value-added chemicals. Meanwhile, solvolysis has gained attention as one of the promising techniques because yield of products is relatively high and the better quality of products can be obtained by using solvolysis compared with the others. Especially, solvolysis by using alcohol solvents such as methanol or ethanol receives more attention because *in-situ* hydrogen is generated from supercritical alcohol, which is essential to cleave C-O bonds. Also, the combination of catalyst and supercritical ethanol is recently applied to the depolymerization of lignin since the catalyst is able to selectively cleave C-O bonds.

In this work, catalytic conversion in supercritical ethanol was conducted to explore i) reaction pathway of benzyl phenyl ether, containing α-O-4 bonds ii) depolymerization of real lignin sources (concentrated strong acid hydrolysis lignin; CSAHL, Protobind lignin; PL) without supplying external hydrogen.

At first, model compound reaction was conducted by using benzyl phenyl ether (BPE, containing α-O-4 bonds) in supercritical ethanol. The yield of

phenol and toluene over carbon-supported catalysts was two times higher than that of phenol and toluene over Al_2O_3-supported catalysts. In addition, Ru catalysts demonstrated the maximum yield of phenol and toluene of 96.4 % among the three different metal catalysts (Ru, Pt and Ni). It was ascribed to the small particle size (about 1.5 nm) with highly dispersed phases. Meanwhile, both the amount of generated H_2 and the amount of alkylated phenols were the highest in supercritical ethanol over 5 wt.% Pt/C among the catalysts, implying that the catalyst promoted alkylation more abundantly.

Secondly, the concentrated strong acid hydrolysis lignin (CSAHL) was used for depolymerization lignin in supercritical ethanol over various catalysts. In case of $MO(30)MgAlO_y$ (M=Co, Ni, and Cu) catalysts, $CuO(30)MgAlO_y$ revealed the highest yield of monoaromatic compounds of 18.4 wt.% because the amount of NH_3 desorbed from the catalyst was the highest among the catalysts. It can be concluded that acid sites is a critical factor for depolymerization of lignin to produce monoaromatic compounds. Meanwhile, as the amount of Cu loading was changed from 10 wt.% to 40 wt.% in $CuO(X)MgAlO_y$, the trend of the yield of monoaromatic compounds showed a volcano shape. Thus, the maximum yield of monoaromatic compounds displayed in $CuO(30)MgAlO_y$, resulting from the highest number of acid sites. When the amount of Cu loading exceeded over 30 wt.%, the number of acid sites decreased, leading to the decrement of the yield of monoaromatic compounds.

The depolymerization of Protobind lignin was conducted in supercritical ethanol over various parameters based on ZSM-5 zeolites such as types of transition metals (Co, Ni and Cu), the amount of Cu loading (5 wt.%, 10 wt.% and 30 wt.%) and the Si/Al_2 ratio (30, 50, 80 and 200). As a result, 10 wt.% Cu/ZSM-5(30) showed the highest yield of monoaromatic compounds of 98.2 wt.% due to the highest acid density (3.2 $mmol/m^2$). As the acid density increased, the yield of monoaromatic compounds increased as well. Thus, the linear correlation between the acid density and the yield of monoaromatic compounds was confirmed. On the basis of the results, it can be summarized that the acid density played a key role in depolymerizing Protobind lignin to convert monoaromatic compounds. Meanwhile, through HSQC NMR analysis, it was identified that depolymerization of Protobind lignin was conducted via hydrogenolysis. Moreover, HSQC NMR signals corresponding to ethylated products were observed with weak intensity, which is consistent with the product analysis. It was also found that the addition of Cu metal plays a promotional role in enhancing the lignin depolymerization.

Keywords: Catalytic depolymerization of lignin, Supercritical ethanol, *in-situ* hydrogen, acid site

Student Number: 2013-30989

Contents

List of Scheme and Tables

List of Figures

Chapter 1. Introduction

1.1 Biomass as a renewable source

Biomass is the most abundant renewable carbon resources so that it is considered as one of the promising alternative chemicals [1, 2]. Because of the depletion of fossil fuels, the production of chemicals from biomass is inevitable [3]. Especially, lignin has significant potential as a good feedstock for the production of valuable chemicals such as BTX, phenols and other aromatics [4, 5]. Therefore, a large amount of bulk and fine chemicals such as aromatic compounds can be acquired from lignin. Indeed, various researches on the production of chemicals from lignin are widely reported. Singh *et al.* reported on the production of substituted phenols and aromatic ethers from Asian lignin via hydrothermal liquefaction [4]. Rajappagowda *et al.* described the selective liquefaction of lignin to value-added phenolic monomers [6].

1.2 Structure of lignin and linkages

Lignocellulosic biomass typically consists of three major components, cellulose, hemicellulose and lignin as shown in Figure 1-1 [7]. Lignin constitutes about 15-35 % of the dry weight lignocellulosic biomass [8]. It fills the spaces between cellulose and hemicellulose to retain strengthen of lignocellulose matrices. It also leads to structural rigidity. Depending on the types of wood, the lignin content in lignocellulosic biomass varies between 17-33 wt.% [9]. The amount of lignin in a plant is followed by softwood > hardwood > grasses. The content of lignin in softwood is about 27-33 wt.%, that of lignin in hardwood is about 18-50 wt.% and that of lignin in grasses is about 17-24 wt.% [10]. Lignin, a randomly cross-linked polymer by using coumaryl (hydroxyphenol unit), coniferyl (guaiacyl unit) and sinapyl alcohols (sinapyl unit), is a three-dimensional amorphous polymer consisting of polyaromatic compounds displayed in Figure 1-2. Meanwhile, the composition of the units in lignin is depending on the wood types. In other words, softwood lignin is composed of 90-95 % of coniferyl units and the others are sinapyl units. Hardwood lignin consists of the equal amount of coniferyl and sinapyl units. In case of grasses, the amount of coniferyl units is 75 %, that of sinapyl is 25% and coumaryl is 5 % [11-13].

Building blocks of lignin are mainly linked by ether bonds (C-O) and carbon-carbon bonds (C-C) such as β-O-4, α-O-4, 4-O-5, β-5, β-1, β-β and 5-5 bonds and their properties and schematic structures are displayed in Table 1-1 and Figure 1-3. The composition of these linkages in lignin varies with the types of wood [14]. Especially, among various ether bonds, β-O-4 is a representative one included in all lignins. In case of hardwood, it contains about 60 % and does in softwood as 40 % [15].

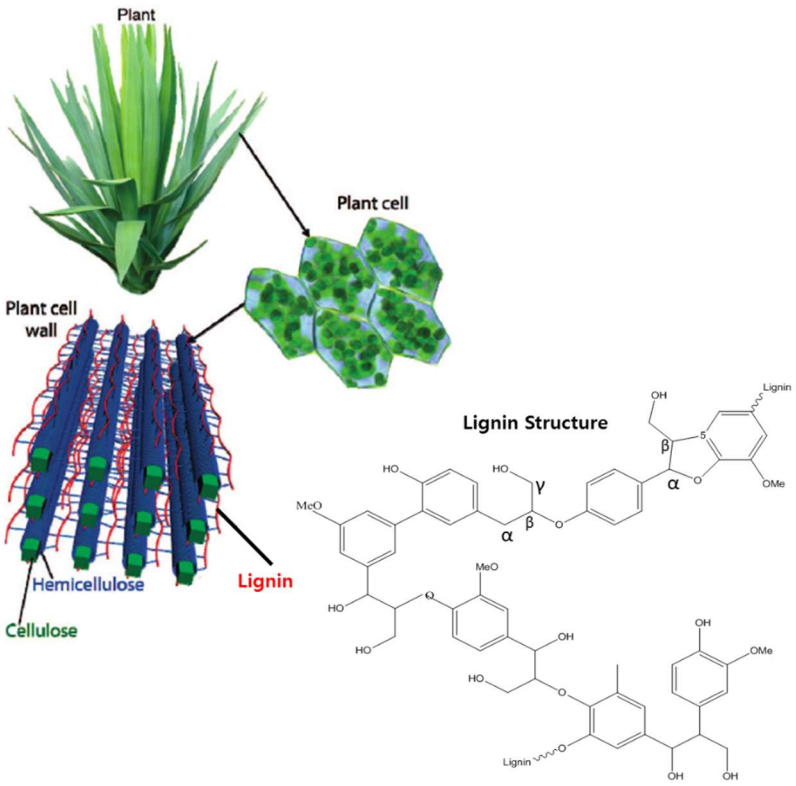

Figure 1-1. Schematic structure of lignin in lignocellulosic biomass [7].

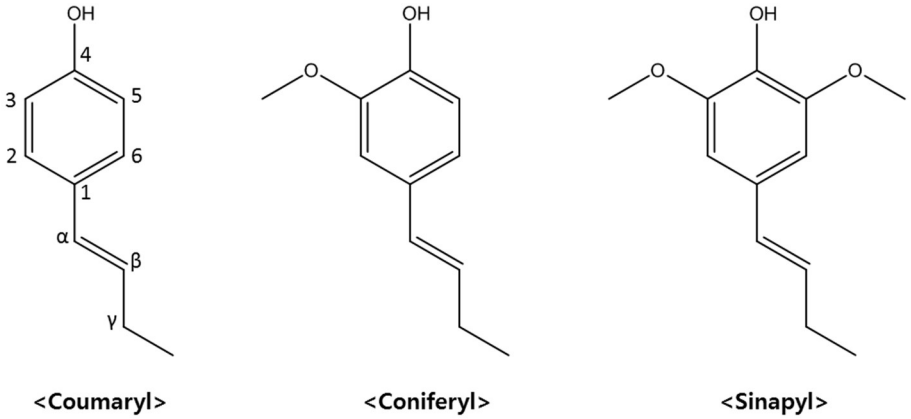

<Coumaryl> <Coniferyl> <Sinapyl>

Figure 1-2. Chemical structure of three primary monomers of lignin [10].

Table 1-1. Proportion of interunit linkages in lignin [15]

Linkages	Softwood (%)	Hardwood (%)
β-O-4	46	60
α-O-4	6-8	6-8
4-O-5	3.5-4	6.5
β-5	9-12	6
β-1	9.5-11	4.5
β-β	7	7
5-5	2	3
Others	13	5

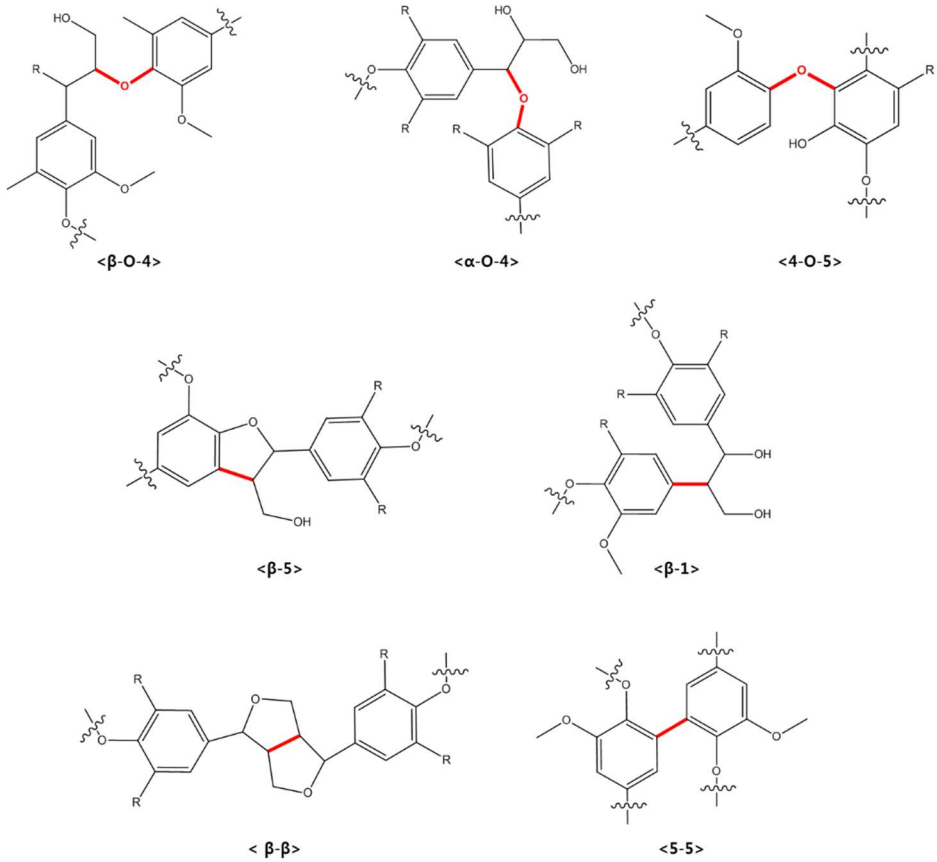

Figure 1-3. Schematic structure of various linkages of lignin [10].

1.3 Valorization of lignin

In pulp industry, lignin is produced about 95 % of every year and it is mostly converted into heat and power sources only [16, 17]. In this respect, as the consideration of the depletion of the fossil fuels, lignin has great potential to be used as a renewable source for value-added chemicals.

For the several decades, the valorization of lignin into chemicals has been developed by using thermochemical processes: gasification, pyrolysis, catalytic cracking, hydrotreatment and solvolysis [2, 14, 18-21]. Figure 1-4 displays these various thermochemical processes depending on temperature and pressure [22]. Gasification and pyrolysis are considered as the easiest ways to convert lignin into chemicals. Meanwhile, hydrotreatment method is another attractive one because it can easily remove ether linkages in lignin subunits so that monoaromatic compounds can be produced [22]. The other attractive method is solvolysis. It is because lignin can be converted into value-added chemicals under relatively lower temperature compared with pyrolysis and gasification. Also, it is useful for preventing repolymerization reaction and reverse reaction [23, 24]. However, it is inevitable to find more efficient ways to get high yield and selectivity of chemicals. For an alternative, catalytic cracking has been widely used for lignin depolymerization because lignin can

be cleaved by applying appropriately selected catalysts [25]. In this respect, the use of this method would be the best way to obtain the high yield of value-added chemicals.

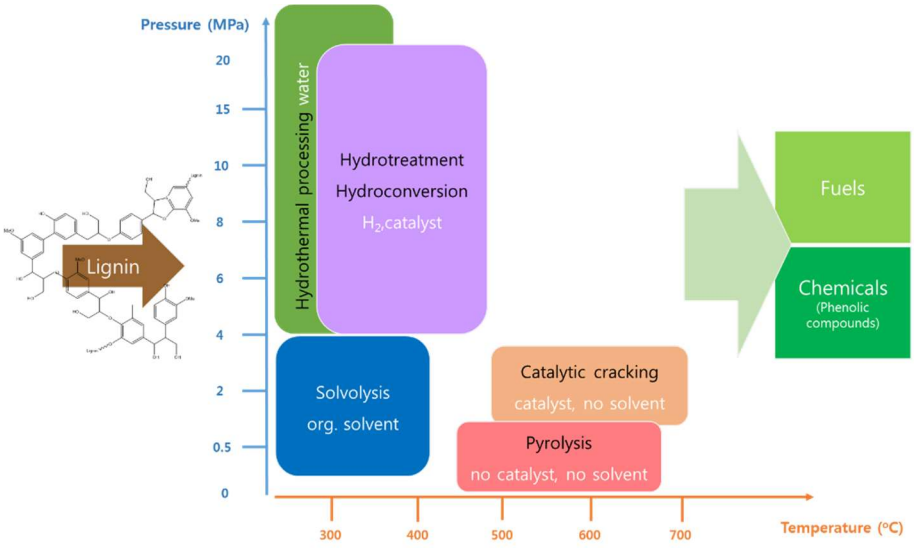

Figure 1-4. Thermochemical processes and (P,T) parameters range for lignin valorization into chemicals [22].

1.4 Catalytic depolymerization of lignin in supercritical fluid

The difficulty of conversion of lignin into value-added chemicals originates from its recalcitrant structure and lots of ether linkages. Therefore, the selective cleavage of C-O bonds is very important to get the high yield of chemicals. To cleave C-O bonds more efficiently, gaseous H_2 is necessary. However, there has been a drawback that gaseous H_2 should be externally supplied. To solve this, catalytic depolymerization of lignin in supercritical fluid has been studied (Figure 1-5). More details will be described in the following section.

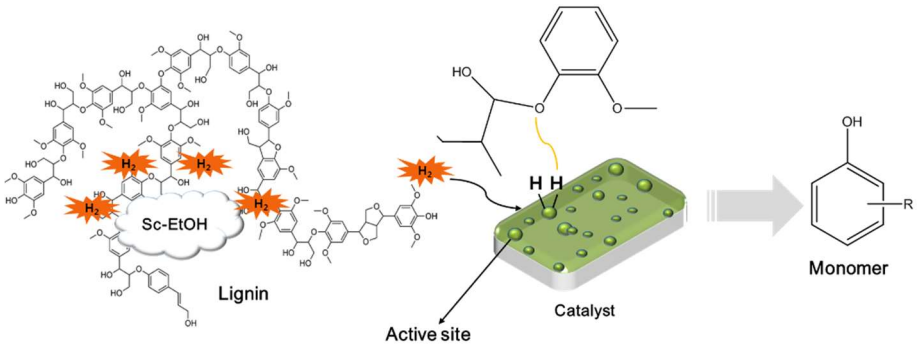

Figure 1-5. Catalytic depolymerization of lignin in supercritical ethanol without supplying external hydrogen.

1.4.1 Supercritical fluids (*in-situ* Hydrogen)

In solvolysis, the solvent typically plays a critical role in obtaining desirable yield and properties. Among various solvents such as water and alcohols (methanol, ethanol and propanol), especially, supercritical alcohol solvents have studied as potential reaction media [26-28]. It is because they can produce *in-situ* hydrogen in supercritical condition. In other words, supercritical alcohol can act not only as a reaction medium but also as a reactant [29]. The mechanism on generation of hydrogen from supercritical alcohol is reported in previous studies (Scheme 1). The first mechanism suggests that α-hydrogen is donated in the form of hydride and electron-deficient species. Another mechanism, similar to the Meerwein-Ponndorf reduction, is composed of alcohol reduction that results in alkoxide ion and proton transfer and then induces α-hydrogen donation and ketone formation [26, 30].

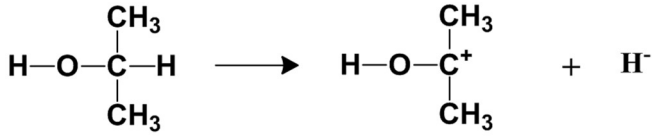

Nakagawa et al [26].

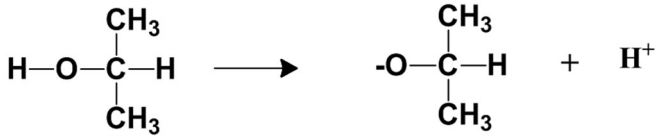

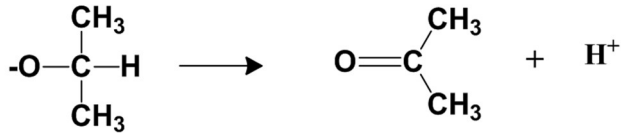

Ross et al [30].

Scheme 1-1. Hydrogen donation mechanisms [26, 30].

1.4.2 Porous metal oxides (PMOs)

Porous metal oxides (PMOs) derived from hydrotalcite-like materials are known for effective catalysts for lignin depolymerization because of no or less formation of char [20]. Generally, they can be synthesized by changing the Mg/Al molar ratio and it can lead to the change of the basicity and acidity of the catalyst [31, 32]. This property is also attractive for lignin depolymerization. Huang *et al*. has reported on the relation between the ratio of (Cu+Mg)/Al and lignin depolymerization [33]. Meanwhile, by substituting Mg^{2+} to another ion such as Cu^{2+}, the property of porous metal oxides (PMOs) can be changed as well; alcohol reforming is catalyzed by using Cu-doped porous metal oxides [34]. Indeed, hydrogen produced from alcohol reforming is used for cleavage of the aromatic ether bonds and further deoxygenation [35].

1.4.3 Zeolites

Zeolites have been proven as efficient catalysts for aromatization of (non)oxygenated feedstocks so that they can be applied for biomass conversion such as lignin depolymerization [36, 37]. Zeolites have their own properties such as great hydrothermal stability, porous structure and controllable acidity, which make them more promising candidate for lignin depolymerization. Especially, ZSM-5 zeolites are known for that they have ideal pore size and acidity for aromatization and catalytic cracking so they are indeed widely used for bio-oil production from biomass [37, 38]. Many studies by using ZSM-5 for lignin depolymerization have been widely reported [39, 40].

1.5 Objectives

Finding alternative chemicals has become more imperative because fossil fuels are depleted. In this respect, biomass conversion from lignin is one of the promising candidates for sustainable resources because lignin has many carbon-based linkages (C-O-C and C-C). The key for lignin depolymerization is closely related to the cleavage of ether linkages in lignin. The cleavage of ether linkages basically requires gaseous hydrogen, which is typically supplied from external site. For the supply of external hydrogen, infra-structure is necessary.

In this regard, the objective of this thesis is to design a catalytic depolymerization system in supercritical ethanol, develop highly effective catalysts, perform lignin depolymerization by using self-generated hydrogen (*in-situ* hydrogen) and understand the role of the various catalysts.

The reaction by using lignin model compound was conducted to understand reaction pathway in supercritical ethanol. Design and synthesis of various catalysts for lignin depolymerization were studied. On the basis of the experiment results, the role of the catalysts had been demonstrated by using various techniques.

Chapter 2. Understanding the catalytic cleavage of C-O linkages in benzyl phenyl ether by using carbon-supported catalysts in supercritical ethanol

2.1 Introduction

Lignin is a three-dimensional amorphous co-polymer, composed of methoxylated phenylpropane structures such as coniferyl, ρ-coumaryl and sinapyl alcohols [11, 41]. Its complex and recalcitrant structure makes lignin hard to cleave into oligomers and/or monomers [42, 43]. Therefore, the selective cleavage of C-O bonds in lignin remains a big challenge. Many methods such as pyrolysis, catalysis and solvolysis have been applied for lignin depolymerization [44-46]. Especially, solvolysis by using alcohol medium such as methanol or ethanol receives more attention because it is possible to conduct delignification without supplying additional hydrogen gas [47]. Indeed, Güvenatam *et al*. has conducted lignin depolymerization in supercritical ethanol without the addition of external hydrogen gas, stating that lignin conversion in supercritical ethanol leads to high yield of monomers [48]. Catalytic cracking can be also attractive process for the selective cleavage of lignin because the reaction is able to be controlled by selecting appropriate

catalyst [19, 49]. Kim *et al*. has claimed that the catalytic depolymerization activity is determined by the amount of acid sites on the catalyst [50].

Meanwhile, among various catalyst supports, carbon materials have been greatly considered as one of the promising catalyst supports because of excellent textural property, highly resistant to acidic and basic environments and relative chemical inertness [51-53]. Indeed, there have been many studies on lignin depolymerization using carbon supported catalyst [54]. Klein *et al*. has studied about the effect of metal loadings on carbon support, types of biomass and their origins of biomass sources on the lignin depolymerization [55]. Song *et al*. has reported on the catalytic conversion of lignosulfonate lignin into phenols by using various catalysts (mainly focused on carbon supported catalysts) [56].

C-O bonds containing α-O-4, β-O-4 and 4-O-5 linkages, are the most abundant types in lignin [15]. α-O-4 linkages are the lowest bond dissociation energy of the aliphatic C-O bonds (218 kJ/mol) so that it is the most active and thermally unstable [57, 58]. Understanding the mechanism of cleavage of C-O bonds is of practical importance to utilize lignin, so benzyl phenyl ether (BPE) containing the chemical linkages which is similar to lignin, is selected as the model compound.

Most of previous researches on BPE concerned about the catalytic effect while a few researches addressed the effect of solvents [59-61]. However, the studies on cleavage of C-O bonds which is performed in the presence of both supercritical fluid and catalyst are not unequivocally established. Therefore, the aim of the study is to investigate the carbon-supported catalysts with various metals (Ru, Pt and Ni) and suggest reaction pathways of decomposition of BPE in the reaction system of supercritical ethanol and catalyst in the absence of external hydrogen.

2.2 Experimental

2.2.1 Chemicals

Lignin model compounds, namely benzyl phenyl ether (BPE, Alfa Aesar, 97 %) and phenol (Sigma-Aldrich, ≥99.5 %) were used as received. For carbon-supported catalysts, 5 wt.% Pt/C and 5 wt.% Ru/C were purchased from Alfa Aesar and used after drying. For synthesis of 10 wt.% Ni/C, $Ni(NO_3)_2 \bullet 6H_2O$ (Alfa Aesar) and activated charcoal (Sigma-Aldrich) were used. In case of Al_2O_3-supported catalysts, Al_2O_3 support was obtained from Sasol Company. $Pt(NH_3)_4 \bullet (NO_3)_2$ (Sigma-Aldrich), $RuCl_2 \bullet xH_2O$ (Alfa-Aesar) and $Ni(NO_3)_2 \bullet 6H_2O$ (Alfa Aesar) were used for metal precursors. Ethanol (Sigma-

Aldrich, 200 proof, ACS reagent, ≥99.5 %) was selected as a reaction medium for the decomposition of model compounds in supercritical condition.

2.2.2 Catalyst preparation

All catalysts were prepared by applying wet impregnation method. Briefly, metal precursor was dissolved in distilled water and added into support material. After impregnation in a rotary evaporator, the catalyst was dried in an oven overnight and calcined at 460 °C for 2 h over Ru and Ni catalysts and at 500 °C for 2 h over Pt catalyst, respectively while flowing nitrogen. The calcined catalysts were then reduced at 150 °C for Ru catalyst, 460 °C for Ni catalyst and 500 °C for Pt catalyst for 2 h in 15% H_2/N_2 condition prior to the reaction.

2.2.3 Characterization

The X-ray diffraction (XRD) patterns were obtained by a powder X-ray diffractometer with Cu Kα radiation (Rigaku Corp.) in an operating mode of 40 kV and 30 mA. The scan step was fixed as 0.02 degree in the range of 10-90 degree. Transmission electron microscope (TEM, JEM-2100F, 200 kV) was applied in order to measure particle size in the sample. The solution prepared by dispersing small amount of catalysts in ethanol was dropped on a carbon-coated Au grid and dried at room temperature.

2.2.4 Experimental setup and procedure

50 mL stainless-steel autoclave was used for benzyl phenyl ether (BPE) decomposition reaction. 0.5 g of BPE and 25 mL of ethanol were charged into the autoclave. Then, 0.2 g of catalyst was loaded into the designed basket (stainless-steel, 500 mesh). The reactor was purged with nitrogen to remove air. Prior to the reaction, nitrogen gas was pressurized to a total pressure 10 bar at room temperature. The autoclave was heated to 270 ^{o}C (12 ^{o}C/min) while stirring at 500 rpm for 3 h. After the reaction, the reactor was quickly quenched to below 130 ^{o}C by using in an ice water. In addition, model compound reaction using phenol as reactant was also identical to previous procedures. The conversion and the selectivity were calculated based on analyzed products and the equations were followed by:

$$\text{X for reactant (\%)} = \frac{\text{(moles of reactant) reacted}}{\text{(moles of reactant) in}} \times 100 \quad (1)$$

$$\text{S for aromatics (\%)} = \frac{\text{(moles of products) formed}}{\text{(moles of reactant) in}} \times 100 \quad (2)$$

$$\text{Y for aromatics (\%)} = (\text{X} \times \text{S}) \times 100 \quad (3)$$

2.2.5 Product analysis

GC-MS (Agilent 6890N, DB-5ms, 30 m x 0.25 mm x 0.25 μm) and GC-FID (Agilent 6890A, DB-5, 60 m x 0.25 mm x 0.25 μm) analysis of liquid product was conducted without any dilution. Fluoranthene was used as an

internal standard (ISTD). The injector and detector temperatures were 310 °C and 320 °C, respectively. The initial oven temperature of the GC was 50 °C for 5 min and the temperature was programmed to increase up to 90 °C (10 °C/min), followed by an increase up to 130 °C (1 °C/min), 220 °C (5 °C/min) and 325 °C (10 °C/min), and then maintained at 325 °C for 10 min. The gaseous product was analyzed by GC to identify and quantify H_2. GC-TCD (Agilent 6890N, Carboxen 1000, 30 m x 0.53 mm x 0.25 μm) was used for analysis. The initial oven temperature was 35 °C for 2 min and the oven was heated to 250 °C at a rate of 10 °C/min for 1 min. The injector temperature was 183 °C and the detector temperature was 250 °C.

2.3 Results and discussion

2.3.1 Decomposition of BPE in supercritical ethanol

The reaction pathways for decomposition of BPE are displayed in Figure 2-1. By cleaving C-O bonds in BPE, aromatic compounds such as toluene and phenol are mainly produced in addition to alkylated phenols (2-ethylphenol and 4-ethylphenol) and other dimers (2-phenylmethyl-phenol and dibenzyl ether) are also formed as by-products. In this work, the decomposition of BPE was performed in supercritical ethanol at 270 °C for 3 h over metal-based catalysts either supported on Al_2O_3 (5 wt.% Ru, 5 wt.% Pt and 10 wt.% Ni) or on carbon

(5 wt.% Ru, 5wt.% Pt and 10 wt.% Ni). As described in Table 2-1, among Al_2O_3-supported catalysts, 5 wt.% Pt/Al_2O_3 shows the highest conversion of BPE (88.2 %), while, the lowest selectivity (23.5 %) for phenol and toluene, leading to the lowest yield of phenol and toluene as 20.7 %. Meanwhile, the conversion of BPE over 5 wt.% Ru/Al_2O_3 is slightly higher than that of BPE over 10 wt.% Ni/Al_2O_3. The selectivity for phenol and toluene over the former is 57.8 % and the latter is 53.9 %, therefore, the yield of phenol and toluene over 5 wt.% Ru/Al_2O_3 is much higher than that for phenol and toluene over 10 wt.% Ni/Al_2O_3 as 46.1 % and 42.3 %, respectively. Although the conversion of BPE over Al_2O_3-supported catalysts is significantly high, the selectivity and the yield of phenol and toluene are relatively low. This can be explained by the high selectivity of dimers such as 2-phenylmethyl-phenol and dibenzyl ether as shown in Figure 2-2.

In case of carbon-supported catalysts, the conversion of BPE over the catalysts increases in the order of 10 wt.% Ni/C (88.7 %) < 5 wt.% Pt/C (93.2 %) < 5 wt.% Ru/C (93.7 %). The selectivity and the yield of phenol and toluene over the catalysts are almost two times higher than those for phenol and toluene over Al_2O_3-supported catalysts. Note that dimer products, which were produced over Al_2O_3-supported catalysts are not observed over carbon-supported catalysts as shown in Figure 2-3. Therefore, it can be concluded that carbon-

supported catalysts are more suitable for decomposition of BPE than Al_2O_3-supported ones. The optimum metal for decomposition of BPE is Ru because the selectivity and the yield of phenol and toluene for both Al_2O_3 and carbon-supported catalysts are the highest.

Figure 2-3 exhibits the result of GC chromatograms of products from decomposition of BPE over the catalysts. In addition to phenol and toluene, the peaks of a variety of alkylated phenols are observed, whereas the peaks of cyclic compounds are rarely detected. The intensity of alkylated phenols increases in the order of 5 wt.% Ru/C < 10 wt.% Ni/C < 5 wt.% Pt/C. According to Sato *et al*., alkylation is catalyzed by protons arising from supercritical water and by increasing the water density, resulting in the enhanced alkylation due to the increment of the concentration of protons [62].

In order to investigate the amount of generated H_2 from the each catalyst, the blank reaction (conducted without reactant) was performed in supercritical ethanol at 270 ^oC for 3 h and the results are shown in Table 2-2. In the blank reaction, the amount of generated H_2 from 5 wt.% Pt/C is the highest, followed by 10 wt.% Ni/C and 5 wt.% Ru/C. It is confirmed that Pt catalyst is significantly reactive for production of H_2, which is in accordance with previous research [63]. Based on the result, it can be concluded that 5 wt.%

Pt/C catalyst in supercritical ethanol can promote alkylation and H_2 production from ethanol more significantly, followed by 10 wt.% Ni/C and 5 wt.% Ru/C.

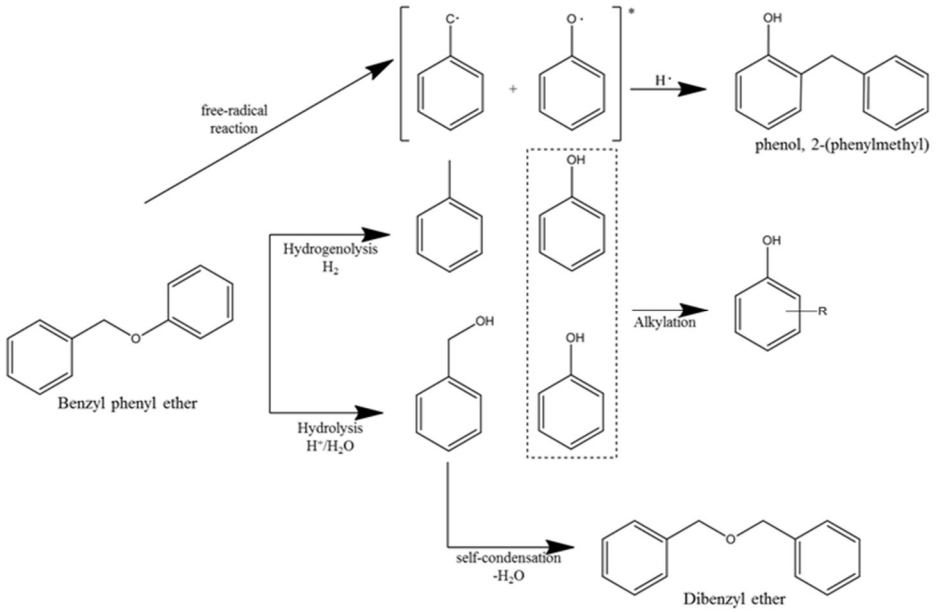

Figure 2-1. Reaction pathways for cleavage of benzyl phenyl ether [64, 65].

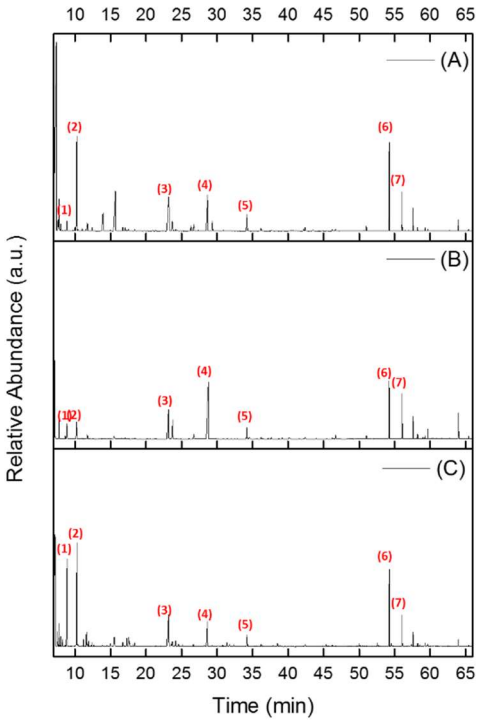

Entry	Compounds	
1	1,1-diethoxy ethane	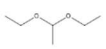
2	Toluene	
3	Phenol	
4	Dibenzyl ether	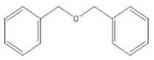
5	2-ethyl phenol	
6	Benzyl phenyl ether	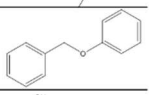
7	Phenol, 2-(phenylmethyl)	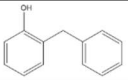

Figure 2-2. GC chromatograms of the products from decomposition of BPE in supercritical ethanol by using (A) 10 wt.% Ni/Al_2O_3, (B) 5 wt.% Pt/Al_2O_3 and (C) 5 wt.% Ru/Al_2O_3.

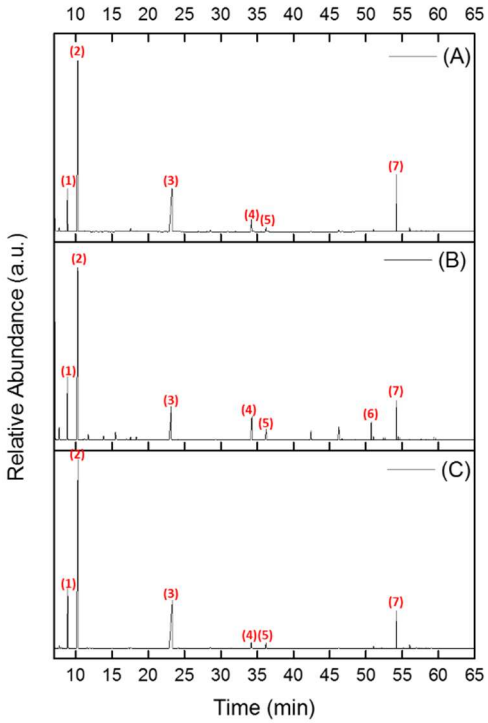

Entry	Compounds	
1	1,1-diethoxy ethane	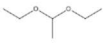
2	Toluene	
3	Phenol	
4	2-ethyl phenol	
5	4-ethyl phenol	
6	2,5-diethylphenol	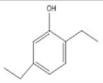
7	Benzyl phenyl ether	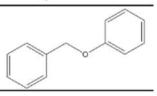

Figure 2-3. GC chromatograms of the products from decomposition of BPE in supercritical ethanol by using (A) 10 wt.% Ni/C, (B) 5 wt.%Pt/C (C) 5 wt.% Ru/C.

Table 2-1. Effect of the various catalysts on the decomposition of BPE at 270 ^{o}C for 3 h

Entry	Catalyst	Conversion (%)	Selectivity (%)			Yield (%)
			Phenol	Toluene	Total	
1	5 wt.% Ru/Al_2O_3	79.8	32.0	25.8	57.8	46.1
2	5 wt.% Pt/Al_2O_3	88.2	19.9	3.6	23.5	20.7
3	10 wt.% Ni/Al_2O_3	78.6	29.5	24.4	53.9	42.3
4	5 wt.% Ru/C	93.7	48.5	54.3	102.8	96.4
5	5 wt.% Pt/C	93.2	25.8	48.2	74.0	69.0
6	10 wt.% Ni/C	88.7	48.8	41.1	89.9	79.9

Table 2-2. The amount of hydrogen gas in supercritical ethanol at 270 °C for 3 h in the absence of reactant

Unit: ppm (x 10^5)

Entry	Catalyst	Blank*
1	5 wt.% Ru/C	1.73
2	5 wt.% Pt/C	5.69
3	10 wt.% Ni/C	4.01

* Blank: reaction w/o BPE (reactant)

2.3.2 Characterization of the catalysts

A series of carbon-supported catalysts with different metals such as Ru, Pt and Ni were prepared and their physical properties were explored. First of all, Figure 2-4. displays the diffraction peaks of as-reduced catalysts. All catalysts show the identical XRD patterns corresponding to amorphous carbon, while the diffraction peaks of metal is only detected in 10 wt.% Ni/C. This result implies that most of metals impregnated on carbon support exist as highly dispersed phases.

HR-TEM images and particle size distributions of the samples are demonstrated in Figure 2-5. A very narrow distribution of particle size in the range of 1 nm to 2.5 nm is observed over 5 wt.% Ru/C with the average Ru particle size of about 1.5 nm, which indicates that the Ru particles in carbon support is highly dispersed. Meanwhile, 5 wt.% Pt/C displays a slightly broad particle size distribution compared to 5 wt.% Ru/C (the range is between 2 nm to 4 nm) with its average particle size of about 2.9 nm, which is marginally larger than the former. Among the three catalysts, 10 wt.% Ni/C shows a significantly broad particle size distribution in the range of 3 nm to 10 nm with the average Ni particle size of about 7.2 nm.

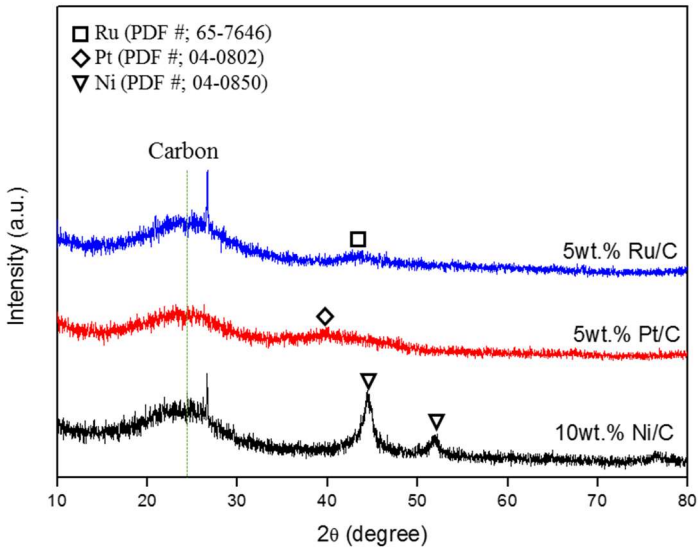

Figure 2-4. XRD patterns of as-reduced catalysts.

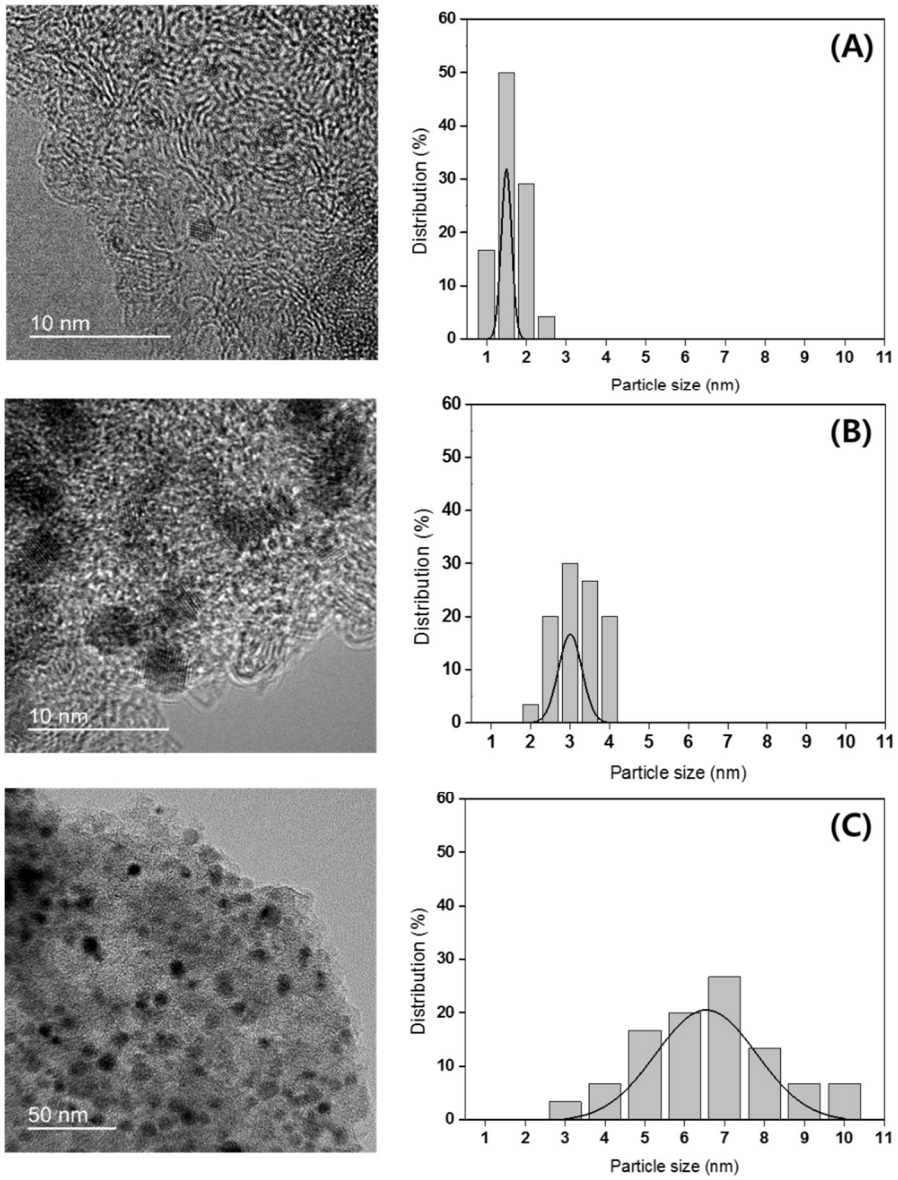

Figure 2-5. HR-TEM and particle size distributions of as-reduced (A) 5 wt.% Ru/C (B) 5 wt.% Pt/C and (C) 10 wt.% Ni/C.

2.3.3 Decomposition of phenol as reactant

In order to understand the side reaction of phenol, the decomposition of phenol in supercritical ethanol was carried out at 270 °C for 3 h over 5 wt.% Ru/C, 5 wt.% Pt/C and 10 wt.% Ni/C. Table 2-3 presents the results of the conversion of phenol over the catalysts.

The conversion of phenol over 5 wt.% Pt/C is 48.1 % and its GC chromatogram is displayed in Figure 2-6. Except for phenol (reactant), a variety of alkylated phenols (2-ethylphenol, 4-ethylphenol and 2,5-diethylphenol) are mainly identified. The peak intensity of alkylated phenols are the highest over 5 wt.% Pt/C among the catalysts (Table 2-4). Note that, 1,1-diethoxy ethane derived from ethanol conversion reaction of the Guerbet type is also produced in all catalysts [66]. Meanwhile, the conversion of phenol over 10 wt.% Ni/C is 38.7 %. Similar to 5 wt.% Pt/C, many of peaks assigned to alkylated phenols are also observed in GC chromatogram in Figure 2-6, whereas the intensity of the peaks over 10 wt.% Ni/C is relatively lower than that of the peaks over 5 wt.% Pt/C, so the peak intensity over 10 wt.% Ni/C is relatively small compared with 5 wt.% Pt/C. It means that alkylation proceeds more actively over the latter than the former. The conversion of phenol over 5 wt.% Ru/C is the lowest as 18.8 %, which results in the lowest peak intensity of alkylated phenols. Meanwhile, the peak intensity of cyclic compounds was too small to quantify

over all catalysts. Based on the result, it can be concluded that among the catalysts, alkylation is the most reactive over Pt catalyst in supercritical ethanol. As mentioned in the previous section, alkylation is promoted by protons and increases with the concentration of protons in supercritical fluid [62].

Based on the result, the plausible reaction pathway is suggested in Figure 2-7. H_2 is generated from supercritical ethanol via reforming by using catalysts and generated H_2 is used for cleavage of C-O bonds in BPE. By cleaving BPE, phenol and toluene are mainly produced in supercritical ethanol. More importantly, 5 wt.% Pt/C in supercritical ethanol promotes alkylation, which leads to the larger production of alkylated phenols. Meanwhile, the extent of alkylation is varied depending on the type of metal on carbon support.

Table 2-3. Decomposition of phenol after reaction at 270 °C for 3 h using carbon-supported catalysts

Entry	Catalyst	Conversion (%)
1	5wt.% Ru/C	18.8
2	5 wt.% Pt/C	48.1
3	10 wt.% Ni/C	38.7

Table 2-4. The area of alkylated phenols from decomposition of phenol by using catalysts at 270 °C for 3 h

Unit: A.U.

Entry	Catalyst	2-ethylphenol	4-ethylphenol	2,5-diethylphenol
1	5wt.% Ru/C	1267	1212	12
2	5 wt.% Pt/C	5126	1565	473
3	10 wt.% Ni/C	3238	1826	341

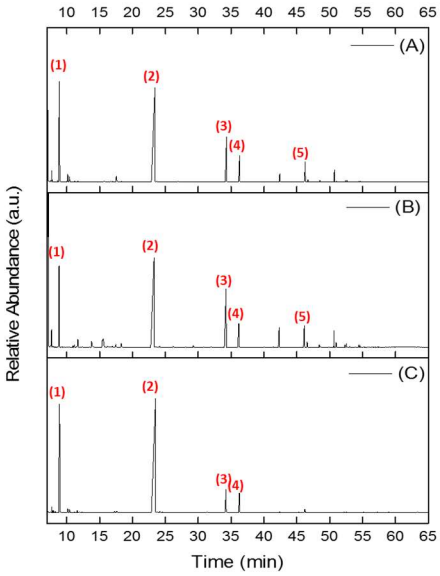

Entry	Compounds	
1	1,1-diethoxy ethane	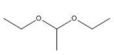
2	Phenol	
3	2-ethyl phenol	
4	4-ethyl phenol	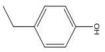
5	2,5-diethylphenol	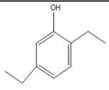

Figure 2-6. GC chromatograms of the products from decomposition of phenol in supercritical ethanol by using (A) 10 wt.% Ni/C, (B) 5 wt.% Pt/C (C) 5 wt.% Ru/C at 270 °C for 3 h.

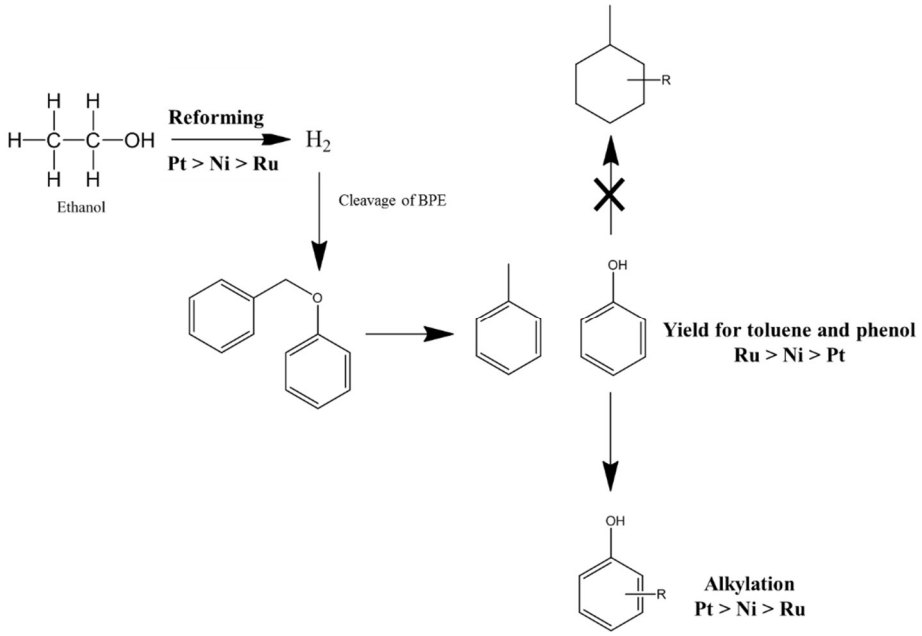

Figure 2-7. Plausible reaction pathways of cleavage of BPE over the catalysts in supercritical ethanol.

Chapter 3. Depolymerization of lignin by using $MO(X)MgAlO_y$ mixed oxide catalyst (M=Co, Ni and Cu) in supercritical ethanol

3.1 Introduction

Finding alternative resources for energy and chemicals becomes imperative as the conventional fossil fuel is rapidly depleted due to the increasing demand [67, 68]. In this respect, lignin can be regarded as one of promising renewable resources for aromatic chemicals because it consists of methoxylated phenylpropane structures such as ρ-coumaryl, coniferyl and sinapyl alcohols [11, 41]. However, the complex and recalcitrant structure of lignin, linked together by C-O and C-C bonds, makes it hard to cleave into oligomers and/or monomers [42, 43]. Especially, the selective cleavage of C-O bonds in lignin remains a big challenge.

There are efforts for valorization of lignin by using various approaches such as hydrolysis, solvolysis, oxidation, pyrolysis and hydrogenolysis [69, 70]. Especially, hydrogenolysis is more attractive method than others to degrade lignin because it is more effective for breaking C-O bond in lignin. It is typically conducted not only in the presence of gas phase hydrogen but also in solvents

such as formic acid, methanol and ethanol under supercritical condition which can easily donate hydrogen. Kleinert *et al*., Xu *et al*. and Huang *et al*. have stated that formic acid plays a role as hydrogen donors under supercritical condition [71-73]. Warner *et al*. also has reported on the hydrogen transfer from supercritical methanol during the lignin depolymerization [34]. Patil *et al*. and Brand *et al*. have claimed that supercritical ethanol can supply *in-situ* hydrogen and, at the same time, can act as a reactant [29, 74].

Meanwhile, there have been several reports on lignin depolymerization in presence of gas phase hydrogen by using heterogeneous catalysts. Song *et al*. has demonstrated that Ni catalyst can convert lignin into monomers via hydrogenolysis and solvolysis [69]. Cu and Ni supported catalysts have also been used to depolymerize and deoxygenate lignin [17, 58]. Porous metal oxides (PMOs) derived from hydrotalcite-like materials ($CuO\text{-}MgAlO_y$) were found to be effective catalyst for lignin depolymerization because of no or less formation of char [20, 66]. However, to the best our knowledge, there have been few researches concerning the analysis of catalysts after lignin depolymerization in supercritical ethanol. For this purpose, we designed a catalyst basket in the reactor to easily separate post-reaction catalyst for analysis. In addition, we aimed at finding the best transition metal among Co,

Ni and Cu and the optimum metal loading for lignin depolymerization under supercritical condition when incorporated into $MgAlO_y$.

3.2 Experimental

3.2.1 Materials and Chemicals

The concentrated strong acid hydrolysis lignin (CSAHL) used in this research was supplied from GS Caltex. The CSAHL was acquired from oak wood (*Quercus acuta*, hardwood) sawdust (C: 46.5 wt.%, H:6.0 wt.%, O: 45.4 %) by using concentrated strong acid hydrolysis process [75]. Thermogravimetric analysis (TGA) indicates that the ash content of CSAHL is about 6.8 wt.%. For catalyst synthesis, $Mg(NO_3)_2•6H_2O$, $Al(NO_3)_3•9H_2O$, $Cu(NO_3)_2•3H_2O$, $Ni(NO_3)_2•6H_2O$, $Co(NO_3)_2•6H_2O$, NaOH and Na_2CO_3 were purchased from Sigma-Aldrich. Ethanol (200 proof, ACS reagent, ≥99.5 %, Sigma-Aldrich) was used as a reaction medium for lignin depolymerization under supercritical condition.

3.2.2 Catalyst preparation

The catalysts, derived from hydrotalcite-like materials, were prepared by using co-precipitation method. Briefly, in order to synthesize $MgAlO_y$, two different kinds of solutions were prepared. Solution A consisted of

$Mg(NO_3)_2 \cdot 6H_2O$ and $Al(NO_3)_3 \cdot 9H_2O$ in distilled water, and solution B did NaOH and Na_2CO_3. Solution B was added into solution A until the pH reached 10 ± 0.05 by keeping the drop-wise rate (1 mL/min) at 65 °C. Synthesized material was calcined at 800 °C for 6 h in a muffle furnace to induce $MgAlO_y$. The detailed procedures are described elsewhere [31, 76-78]. In case of MO-$MgAlO_y$, solution A containing three precursors (M, Mg, Al) was used and the other procedures were exactly the same as described above. The product was calcined at 460 °C for 6 h in a muffle furnace to induce $MO(X)MgAlO_y$. The final material was denoted to $MO(X)MgAlO_y$ (M=Co, Ni and/or Cu, X=10, 20, 30, and 40 wt.% based on metal (M)). In case of Co and Ni, the amount of metal was fixed as 30 wt.%. Typically, the molar ratio of M^{2+}/M^{3+} in hydrotalcites (HTs) is 2/1; here M^{2+} originally stands for Mg ions and M^{3+} does Al ions. In this research, M^{2+} is partially substituted with Co, Ni or Cu ions, so that the molar ratio of M^{2+}/M^{3+} remains constant as 2/1.

3.2.3 Characterization

The total inorganic content was measured by using a TA Instruments Q50 TGA in the temperature range of 50-800 °C at a rate of 10 °C/min in air flow (100 mL/min). Inductively coupled plasma-atomic emission spectroscopy (ICP-AES) was used (PerkinElmer/Optima-4300 DV) to confirm the metal

contents (Mg, Al, Co, Ni and Cu) of prepared catalysts. The weight of the each sample was about 0.03 g, and the sample was dissolved in 5 mL aqua regia. Textural properties of the catalysts were measured using N_2 physisorption apparatus (Micrometritics ASAP 2010). The total surface area of the samples was obtained by the BET method. The pore volume and pore size distributions were measured from the desorption branches of the isotherms using BJH methods. The powder X-ray diffraction (XRD) experiment was performed on a high power X-ray diffractometer (Rigaku Corp.) using Cu Kα as a radiation source at 40 kV and 30 mA. The scan step was fixed as 0.02 degree in the range of 10-90 degree. Temperature programmed desorption of NH_3 (NH_3-TPD) was carried out for the as-calcined catalysts. After pretreatment at 400 ^oC for 1 h under a flow of He (50 sccm), 5 % NH_3 was introduced to 0.03 g of the sample at 50 ^oC for 0.5 h. After purging with He to remove physisorbed NH_3, the temperature was increased from 50 ^oC to 430 ^oC at 10 ^oC/min under flowing He. The desorbed gas (NH_3) was analyzed by a thermal conductivity detector (TCD) (BEL JAPAN INC.).

3.2.4 Catalytic activity measurement

Lignin depolymerization reaction was conducted in a 50 mL stainless-steel high pressure autoclave. The autoclave was filled with 0.5 g of lignin in 25 mL

ethanol. 0.3 g of catalyst was loaded into the designed basket (stainless- steel, 500 mesh). 0.0013 g of fluoranthene was also added as an internal standard. The reactor was sealed and purged with nitrogen several times to remove oxygen. Before the reaction, 10 bar nitrogen at room temperature was loaded into the reactor. Then, the reaction mixture was heated to the desired temperature while stirring at 500 rpm for 40 min. After the reaction, the reactor was quickly quenched below 150 °C by using ice water to cool to room temperature. The yield (Y) of monomers was calculated by following equations:

$$\text{Y (wt.\%)} = \frac{\text{weight of monomers (quantified by GC} - \text{FID)}}{\text{weight of ash free lignin}} \times 100$$

3.2.5 Product analysis

The liquid phase product mixture was analyzed by an Agilent 6890N GC equipped with a DB-5ms column (30 m x 0.25 mm x 0.25 μm) with a mass spectrometer to identify products. Meanwhile, the same liquid phase product was also injected into an Agilent 6890A GC together with a flame ionization detector (FID) with a DB-5 column (60 m x 0.25 mm x 0.25 μm) for the quantification of the products. The liquid product analysis was performed by using as-produced sample, in other words, without any dilution.

3.3 Results and discussion

3.3.1 Effect of MO(X)MgAlO$_y$ mixed oxide catalysts (M=Co, Ni and Cu) on lignin depolymerization

3.3.1.1 Analysis of as-calcined MO(X)MgAlO$_y$ samples

Table 3-1 provides the ICP and N_2 physisorption results of the as-calcined catalysts. Theoretical value of M^{2+}/Al^{3+} is about 2 and the experimental value is between 1.81 and 1.89, meaning that the result of this experiment corresponds with the theoretical one. In case of metal loading, the value was fixed as 30 wt.%. Almost 10 wt.% of metal is over loaded compared with theoretical value except for Co metal. BET surface area of Co_3O_4(30)MgAlO$_y$ is about 198 m^2/g and that of NiO(30)MgAlO$_y$ is about 194 m^2/g, which are slightly larger than that of CuO(30)MgAlO$_y$ (170 m^2/g). The XRD patterns of MO(30)MgAlO$_y$ are displayed in Figure 3-1. The peaks arising from MgO phase are primarily shown in all catalysts and the broad XRD patterns of each transition metal oxides are displayed, indicating that Co, Ni or Cu oxides exist in the amorphous form or highly dispersed state. Figure 3-2 displays the NH_3-TPD profiles of MO(30)MgAlO$_y$. According to the previous study, the NH_3 desorbed below 300 ^oC is regarded as one from NH_3 adsorbed on the weak acid sites of catalyst [79]. When the number of weak acid sites is counted by integrating the amount of NH_3 desorbed up to 300 ^oC, the order is in the following: CuO(30)MgAlO$_y$ > NiO(30)MgAlO$_y$ > Co_3O_4(30)MgAlO$_y$. This result is in accordance with that

of Robinson who claimed that the catalyst containing Cu has a higher number of acid sites than the Ni-containing one, indicating that copper oxides provide new acid sites [80].

Table 3-1. Results of ICP-AES and N_2 physisorption of the catalysts

Entry	Catalyst	ICP-AES		N_2 physisorption	
				As-calcined	Post-reaction
		$M^{2+,a}/M^{3+,b}$	M (wt. %[c])	S_{BET} (m^2/g)	S_{BET} (m^2/g)
1	$MgAlO_y$	2.17	-	170	135
2	$CuO(10)MgAlO_y$	1.78	11.1	171	47
3	$CuO(20)MgAlO_y$	2.00	21.3	166	58
4	$CuO(30)MgAlO_y$	1.81	34.5	170	100
5	$CuO(40)MgAlO_y$	1.98	43.4	172	105
6	$Co_3O_4(30)MgAlO_y$	1.89	31.9	198	-
7	$NiO(30)MgAlO_y$	1.82	33.1	194	-

[a] M^{2+}: Mg and Co, Ni or Cu ions

[b] M^{3+}: Al^{3+}

[c] M: CuO, Co_3O_4 and/or NiO

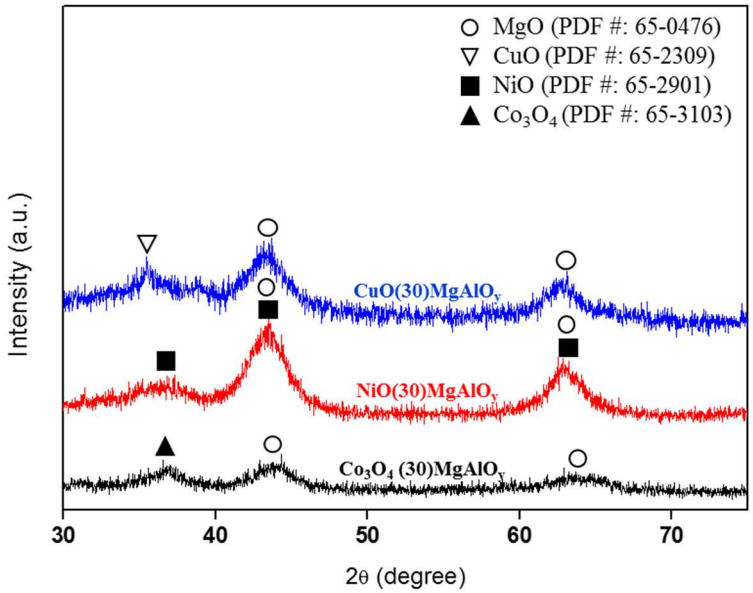

Figure 3-1. XRD patterns of as-calcined MO(30)$MgAlO_y$ (M= Co, Ni and Cu).

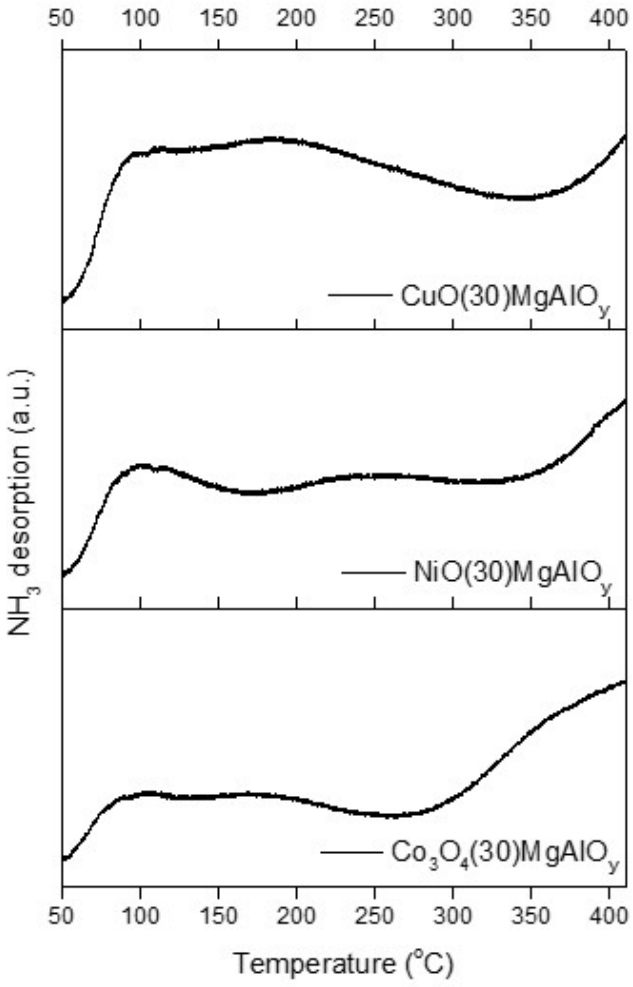

Figure 3-2. NH_3-TPD spectra of $MO(30)MgAlO_y$ (M= Co, Ni and Cu).

3.3.1.2 Lignin depolymerization over MO(X)MgAlO$_y$

To estimate catalytic performance, lignin depolymerization reaction was performed in supercritical ethanol over both without catalyst (blank reaction) and MO(30)MgAlO$_y$ at 400 ^oC for 4 hours. MO stands for transition metal oxides such as Co_3O_4, NiO and CuO and the amount of metals loaded is all the same as 30 wt.%. The total yield of monoaromatic compounds was obtained by adding up the yield of 19 different monomeric products (Figure 3-3) such as γ-valerolactone, phenol, benzyl alcohol, o-cresol, ρ-tolualdehyde, guaiacol, 4-methyl benzyl alcohol, 2-ethyl phenol, 2-methyl benzyl alcohol, γ-heptalactone, 4-ethyl phenol, creosol, 2-propyl phenol, 4-ethyl guaiacol, syringol, 4-propyl guaiacol, 1,2,4-trimethoxy benzene, 3,4,5-trimethoxy toluene and ethyl vanillate. Most of the monoaromatic compounds are oxygen-containing aromatic rings resulting from the cleavage of the β-O-4 linkage or hydrogenolysis of lignin, indicating that the combination of catalyst and supercritical ethanol is effective for the lignin depolymerization without supplying external hydrogen. In addition, there is significant amount of furans which are not counted in the monoaromatic compounds. [66]. Table 3-2 demonstrates the yield of monoaromatic compounds quantified from GC-FID analysis. In case of blank reaction, the yield of monoaromatic compounds is 1.0 wt.%, acquired by adding up only 6 monomers such as benzyl alcohol, o-cresol,

guaiacol, 4-methyl benzyl alcohol, 4-ethyl phenol, 2-propyl phenol among 19 monomers. The result indicates that existence of the catalyst definitely affects improvement of monoaromatic yield. Meanwhile, the yield of monoaromatic compounds over $CuO(30)MgAlO_y$ is the highest as 18.4 wt.%, followed by $NiO(30)MgAlO_y$ of 10.8 wt.% and $Co_3O_4(30)MgAlO_y$ of 10.0 wt.%. Figure 3-4(A) presents the distributions of selected monoaromatic compounds identified and quantified by GC-FID analysis. Creosol, ρ-tolualdehyde, phenol and syringol are the major components in all catalysts. The yield of monoaromatic compounds is well related to the number of acid sites as shown in Figure 3-2, leading to the conclusion that $CuO(30)MgAlO_y$ demonstrated the higher monoaromatic yield due to the higher number of acid sites among Ni, Co and Cu. In conclusion, copper metal might be the most appropriate metal among three kinds of transition metals for lignin depolymerization reaction.

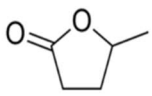	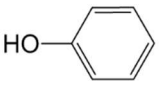	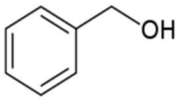	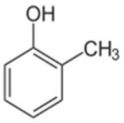
1. g-valerolactone	2.Phenol	3. Benzyl Alcohol	4. o-Cresol
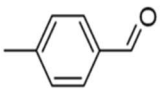	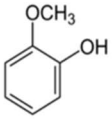	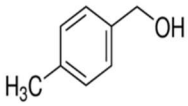	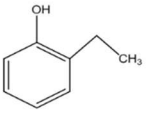
5. p-tolualdehyde	6. Guaiacol	7. 4-methylbenzylalcohol	8. 2-ethylphenol
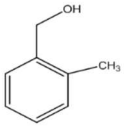	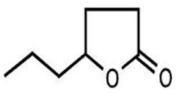	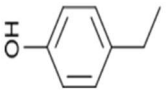	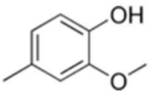
9. 2-Methyl benzylalcohol	10. g-heptalactone	11. 4-ethylphenol	12. Creosol
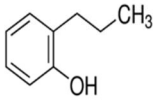	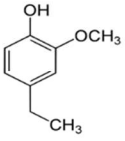	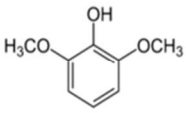	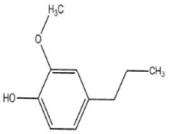
13. 2-propylphenol	14. 4-ethylguaiacol	15. Syringol	16. 4-propyl Guaiacol
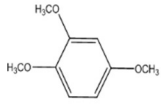	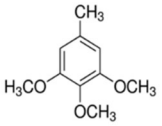	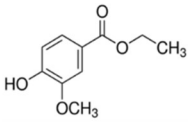	
17. 1,2,4-trimethoxy benzene	18. 3,4,5-trimethoxy toluene	19. Ethyl vanillate	

Figure 3-3. Obtained 19 different monoaromatic compounds from CSAHL.

Table 3-2. The yield of monoaromatic compounds over the catalysts

Entry	Catalyst	Yield of monoaromatic compounds (wt.%)
1	None	1.0
2	$MgAlO_y$	5.7
3	$CuO(10)MgAlO_y$	10.7
4	$CuO(20)MgAlO_y$	14.5
5	$CuO(30)MgAlO_y$	18.4
6	$CuO(40)MgAlO_y$	15.5
7	$Co_3O_4(30)MgAlO_y$	10.0
8	$NiO(30)MgAlO_y$	10.8

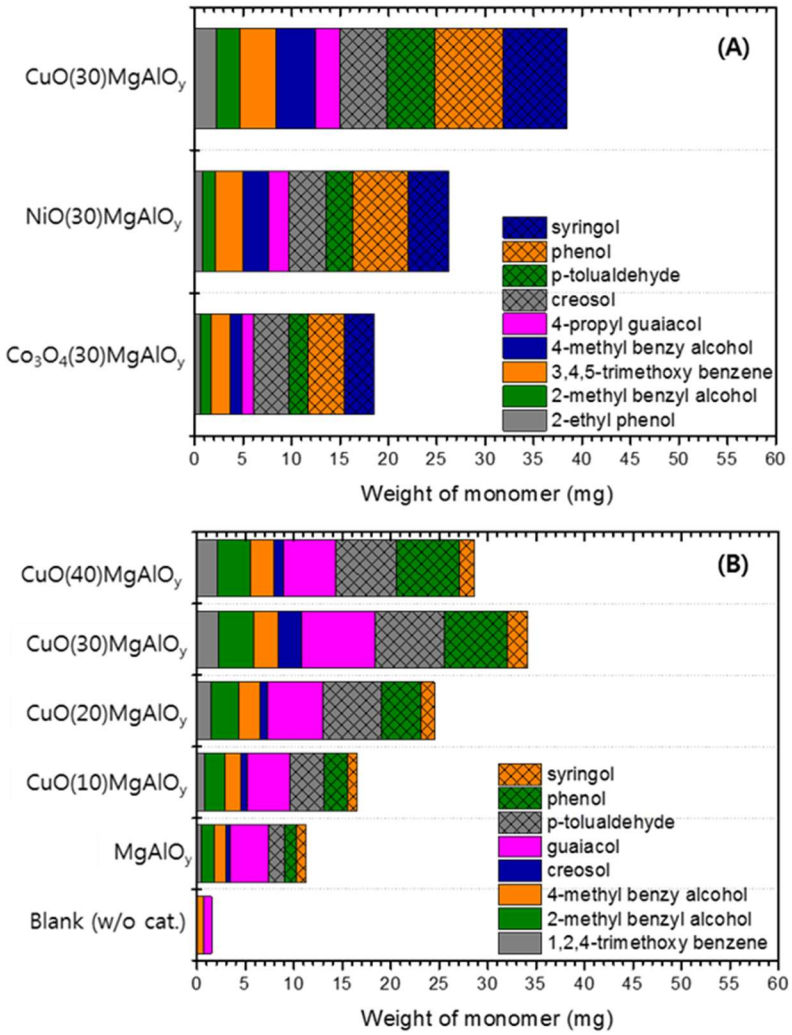

Figure 3-4. Trends of monoaromatic compounds over (A)MO(30)MgAlO$_y$ (M= Co, Ni and Cu) and (B)Blank, MgAlO$_y$ and CuO(X)MgAlO$_y$ (X=10, 20, 30 and 40 wt.%).

3.3.2 Effect of Cu loadings in CuO(X)MgAlO$_y$ on lignin depolymerization

3.3.2.1 Analysis of as-calcined CuO(X)MgAlO$_y$ catalysts

Table 3-1 gives the information of ICP analysis of the catalysts. It is not much difference between the experimental values obtained from ICP-AES and the theoretical ones of M^{2+}/M^{3+} and MO, since the error is within 12 %. Table 3-1 also shows BET surface area of MgAlO$_y$, CuO(10)MgAlO$_y$, CuO(20)MgAlO$_y$, CuO(30)MgAlO$_y$ and CuO(40)MgAlO$_y$ catalysts. The samples have BET surface area of 166 – 172 m^2/g implying that there is no remarkable change in BET surface area even though Cu loading is varying up to 40 wt.%. Figure 3-5(A) demonstrates the XRD patterns of as-calcined catalysts. MgAlO$_y$ catalyst only shows the peaks arising from MgO phase. With increasing Cu loading, the peaks assigned to MgO phase become broad and small probably because of the decrease in MgO amount. Samples with 30 wt.% and 40 wt.% of Cu loading show very broad CuO peak around at 36.9 °, meaning that highly dispersed states of CuO exist in the samples although CuO phase is hardly seen up to 20 wt.% of Cu loading. Interesting to note is that there is no evidence of the Al_2O_3 related phases in XRD, indicating that they exist in small crystallites or amorphous form so that they may not be detected by XRD [81]. In order to measure the acid sites of the catalysts, NH_3-TPD analysis was conducted as displayed in Figure 3-6. The desorption feature of

all catalysts are almost similar which have weak acid sites as evidenced by the NH_3 desorption peak from 100 ^oC to 300 ^oC. Among the catalysts, the amount of weak acid sites is the highest over $CuO(30)MgAlO_y$ as 0.644 mmol/g followed by $CuO(20)MgAlO_y$ (0.422 mmol/g) ≈ $CuO(40)MgAlO_y$ (0.396 mmol/g) > $CuO(10)MgAlO_y$ (0.254 mmol/g). NH_3-TPD result clearly indicates that $CuO(30)MgAlO_y$ has the maximum acid sites among the catalysts.

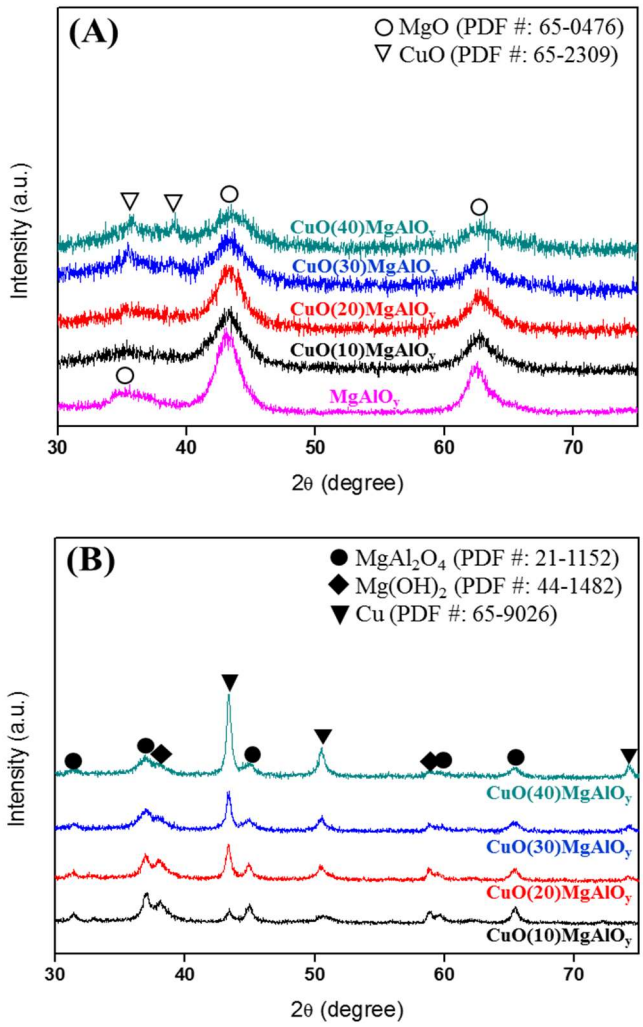

Figure 3-5. XRD patterns of the catalysts (A)as-calcined (B)after lignin depolymerization reaction.

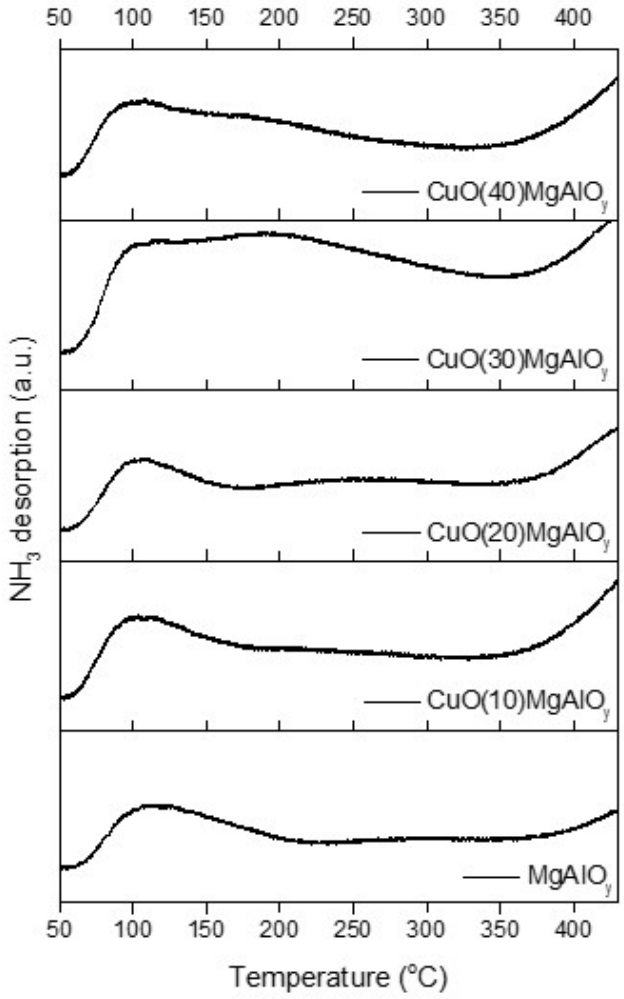

Figure 3-6. NH_3-TPD spectra of the catalysts.

3.3.2.2 Catalytic effect on lignin depolymerization

Lignin depolymerization reaction was conducted in supercritical ethanol to evaluate the effect of Cu loadings in the catalysts at 400 ^{o}C for 4 hours. Table 3-2 displays the yield of monoaromatic compounds calculated from GC-FID result. $MgAlO_y$ demonstrates the lowest monoaromatic yield of 5.7 wt.%. With increasing Cu loading up to 30 wt.%, the yield of monoaromatic compounds gradually increased upto 18.4 wt.%. However, $CuO(40)MgAlO_y$ results in the lower yield (15.5 wt.%) than $CuO(30)MgAlO_y$, indicating that the higher Cu loading than 30 wt.% does not help increasing the yield. Figure 3-4(B) depicts the distributions of selected monoaromatic compounds over $MgAlO_y$ and Cu-containing catalysts quantified by GC-FID. Among various monoaromatic compounds, guaiacol, ρ-tolualdehyde and phenol are the major compounds in all catalysts. Based on this result, it can be summarized that the monoaromatic yield has a close relationship with the number of acid sites, determined by the loading of copper metals.

3.3.2.3 Analysis of post-reaction CuO(X)MgAlO$_y$ catalysts

After lignin depolymerization reaction, the color change of the catalyst (from green to brown) was observed because of the reduction of CuO to Cu due to the *in-situ* H_2 generation (not shown). N_2 physisorption and XRD analysis were conducted for the post-reaction catalysts to understand the change in the physical properties after reaction. As presented in Table 3-1, BET surface area of MgAlO$_y$ decreased from 170 m^2/g to 135 m^2/g after reaction. Moreover, all CuO(X)MgAlO$_y$ catalysts show the significant decrease in BET surface area after reaction. Note that in case of CuO(30)MgAlO$_y$ and CuO(40)MgAlO$_y$, the extent of decrement was less than the others, i.e. 170 m^2/g to 100 m^2/g and 172 m^2/g to 105 m^2/g, respectively. It can be summarized that the textural properties of the CuO(X)MgAlO$_y$ catalysts were changed after reaction, resulting in the substantial decrease of BET surface area. Figure 3-5(B) displays the XRD patterns of the post-reaction catalysts with various Cu loadings. The XRD patterns of all post-reaction catalysts clearly exhibit the highly crystalline of Cu, $Mg(OH)_2$ and $MgAl_2O_4$ phases. First of all, MgO phase was transformed into $Mg(OH)_2$ and $MgAl_2O_4$. We think that such change gives rise to the significant decrease in BET surface area after reaction. Metallic Cu phase at 43.3 ^{o} and 50.5 ^{o} is formed by the reduction of CuO due to *in-situ* hydrogen donated from supercritical ethanol. With increasing the Cu loading up to 30 wt.%, there is a

gradual increase in the peak intensity of Cu phase at 43.3 °. However, at Cu loading of 40 wt.%, more remarkable increase in Cu peak intensity (area: 298 vs. 490) was observed, resulting from the sintering during the reaction, which can account for decrease in monoaromatic yield.

Chapter 4. Depolymerization of Protobind lignin to produce monoaromatic compounds over Cu/ZSM-5 catalyst in supercritical ethanol

4.1 Introduction

Lignocellulosic biomass is regarded as an attractive alternative feedstock to fossil fuels to enable sustainable energy security [82]. Especially, lignin consists of three major phenylpropane units, (guaiacyl alcohol, syringyl alcohol and p-coumaryl alcohol) which are linked by C-C and C-O bonds [83-85]. Because of such unique structure, lignin has the potential to replace the fossil resources in the near future because it can produce value-added chemicals by cleaving C-O bonds. In order to depolymerize and deoxygenate lignin effectively, various thermochemical approaches such as hydrogenolysis, gasification, solvolysis and catalytic cracking have been widely used [6, 56, 86, 87]. Especially, solvolysis using alcohol solvents such as methanol and ethanol as reaction medium is considered as a promising method for lignin depolymerization because it is able to depolymerize and/or deoxygenate without supplying any external hydrogen [33, 43, 48, 74]. Meanwhile, the combination of catalysts with supercritical ethanol is inevitable since catalyst

is able to selectively cleave C-O bonds in lignin. [17, 54, 61]. In current work, we applied zeolite to the catalytic lignin depolymerization in supercritical ethanol because of porous structure, controllable acidity and ability to confine active metal species. [38, 88, 89]. Especially, ZSM-5 zeolites are suitable for aromatization and cracking reaction because they have ideal pore size and acidity for the reaction [90, 91]. Due to such several advantages, various researches by using ZSM-5 have been widely reported. Singh *et al*. has claimed that HZSM-5 and Ni doped HZSM-5 catalysts are efficient for hydrodeoxygenation of lignin [92]. Milovanović *et al*. has reported on the depolymerization of various lignins by using NiO/HZSM-5 [40]. Mullen *et al*. has demonstrated the role of potassium ion exchange in ZSM-5 for biomass conversion [93]. However, even though many researches have used ZSM-5 for lignin depolymerization, the yield of monoaromatic compounds is still not high enough. Therefore, acquiring the high yield of monoaromatic compounds by finding the optimum catalyst is one of the important challenges.

In this respect, the aim of the work is to increase the yield of monoaromatic compounds by depolymerizing Protobind lignin in supercritical ethanol over ZSM-5-supported catalysts. Various parameters such as catalysts, temperature and time were investigated. In addition, the types of transition metals, the loading of metal and the Si/Al_2 ratio of ZSM-5 were also explored.

4.2 Experimental

4.2.1 Materials and Chemicals

Protobind 1000 alkali lignin (PL) was supplied from Eindhoven University. PL was produced from wheat straw (sulfur-free lignin with less than 4 wt.% carbohydrates and less than 2 wt.% ash) by using soda pulping process [66]. For catalyst synthesis, $Cu(NO_3)_2•3H_2O$, $Ni(NO_3)_2•6H_2O$, $Co(NO_3)_2•6H_2O$, were purchased from Alfa Aesar. In case of catalytic support materials, activated charcoal was purchased from Sigma-Aldrich and the commercial NH_4 form ZSM-5 zeolites were purchased from Alfa Aesar: (Si/Al_2 = 30, 50, 80 and 200). Ethanol (Sigma-Aldrich, 200 proof, ACS reagent, ≥99.5 %) was chosen as a reaction medium for depolymerization of lignin in supercritical condition. Tetrahydrofuran (Reagent Plus ≥ 99.0 %, stabilized with butylated hydroxytoluene) and deuterated dimethyl sulfoxide-d_6 (containing TMS) were purchased from Sigma-Aldrich for the post-treatment of liquid products and NMR analysis, respectively.

4.2.2 Catalyst preparation

Commercial activated carbon support was used as-received form, whereas NH_4 ZSM-5 was used after calcination at 550 ^oC for 3 h to induce H ZSM-5 form. Except for $CuO(30)MgAlO_y$, all catalysts were synthesized by applying

wet impregnation method. Metal precursor was dissolved in deionized water and the solution was put into support material and stirred at room temperature for 30 min. Metal was impregnated onto each support by using a rotary evaporator, and then the catalyst was dried in an oven overnight. All prepared catalysts were calcined in a muffle furnace at 500 ^{o}C (Co catalyst) and 460 ^{o}C (Cu and Ni catalysts) for 2 h, respectively. Prior to reaction, the calcined catalysts were reduced at the same condition in 15% H_2/N_2 flow. The reduced catalyst was designated as X wt.% M/support; X = loading of the metal, M = transition metal, support = C or ZSM-5(ratio=30, 50, 80 and 200). In order to synthesize CuO(30)$MgAlO_y$, co-precipitation method was applied and the details were described in our previous research [81, 94-96].

4.2.3 Characterization

Inductively coupled plasma-atomic emission spectroscopy (ICP-AES) was used (SHIMADZU/ICPE-9000) to confirm the metal contents (Si, Al, Co, Ni and Cu) of prepared catalysts. The samples were analyzed by using acid digestion (aqua regia and perchloric acid). Physical properties of the catalysts were analyzed by using N_2 physisorption apparatus (Micrometritics ASAP 2010) at constant temperature (77K). Prior to analysis, all samples were pretreated at 250 ^{o}C for at least 4 h under vacuum condition. The powder X-ray

diffraction (XRD) analysis was conducted on a high power X-ray diffractometer (Rigaku Corp.) using Cu Kα as a radiation source at 40 kV and 30 mA. The scan step was fixed as 0.02 degree in the range of 10-90 degree. Temperature programmed desorption (TPD) of NH_3 was carried out by using BEL CAT II (JAPAN). Prior to the analysis, 0.03 g of sample was heated at 300 ^oC for 1 h under a He flow to get rid of adsorbed impurities. After cooling to 60 ^oC, the sample was saturated with 4.96 % NH_3/He. The physisorbed NH_3 was removed by purging of He flow at 100 ^oC. After the sample was cooled down to 60 ^oC and the TCD signal was stabilized, the TCD signal was recorded with increasing the temperature from 60 ^oC to 550 ^oC at a rate of 10 ^oC/min under a flow of He. The surface morphology of the catalysts was explored by using FE-SEM (field emission-scanning electron microscopy, MERLIN compact, ZEISS). HSQC (Heteronuclear signal quantum coherence) analysis was conducted by using 850 MHz Cryo NMR (AVNACE III HC, Bruker, German). The product was dried at 105 ^oC in an oven overnight and dissolved in 900 μL of deuterated dimethyl sulfoxide d_6 prior to HSQC-NMR analysis.

4.2.4 Catalytic activity measurement

The catalytic depolymerization of lignin was conducted in a 50 mL stainless-steel high pressure autoclave. The reactor was filled with 0.5 g of

Protobind lignin in 25 mL ethanol. 0.3 g of sieved catalyst (425 μm - 600 μm) was loaded into the designed stainless-steel basket with 500 mesh. 0.0013 g of fluoranthene as an internal standard was also added into the reactor. The reactor was sealed and purged with nitrogen several times to get rid of oxygen. Prior to the reaction, 10 bar nitrogen at room temperature was pressurized into the reactor. Then, the reaction mixture was heated to the desired temperature (12 °C/min) for the desired time while stirring at 500 rpm. After the reaction, the reactor was rapidly quenched below 130 °C by using an ice water bath. The yield (Y) of monoaromatic compounds was calculated by following equations:

$$\text{Y (wt.\%)} = \frac{\text{weight of monomers (quantified by GC} - \text{FID)}}{\text{weight of ash free lignin}} \times 100$$

4.2.5 Product analysis

GC-MS (Agilent 6890N, DB-5ms, 30 m x 0.25 mm x 0.25 μm) and GC-FID (Agilent 6890A, DB-5, 60 m x 0.25 mm x 0.25 μm) analysis of liquid product was conducted without any dilution. Fluoranthene was used as an internal standard (ISTD). The injector and detector temperatures were 310 °C and 320 °C, respectively. The initial oven temperature of the GC was 50 °C for 5 min and the temperature increased up to 90 °C at 10 °C/min, followed by an increase up to 130 °C (1 °C/min), 220 °C (5 °C/min) and 325 °C (10 °C/min) for 10 min. The gaseous product was analyzed by GC to quantify H_2. GC-TCD

(Agilent 6890N, Carboxen 1000, 30 m x 0.53 mm x 0.25 μm) was used for analysis. The initial oven temperature was 35 °C for 2 min and the oven was heated to 250 °C at a rate of 10 °C/min for 1 min. The injector temperature was 183 °C and the detector temperature was 250 °C.

4.3 Results and discussion

4.3.1 Screening of the reaction parameters

Lignin depolymerization by using Protobind lignin was performed over various parameters such as catalysts, temperature and time in supercritical ethanol in order to find the optimum reaction conditions. The total yield of monoaromatic compounds is acquired by adding up the each yield of 12 monoaromatic compounds including phenol, toluene, m-xylene, benzyl alcohol, 2-ethylphenol, ethylbenzene, guaiacol, syringol, o-cresol, 4-ethylphenol, benzaldehyde, 1,2,4-trimethoxybenzene. Table 4-1 shows the yield of monoaromatic compounds over the catalysts such as 10 wt.% Ni/C, CuO(30)$MgAlO_y$ and 10 wt.% Ni/ZSM-5(200) at 400 °C for 4 h in supercritical ethanol (Entry 1, 3 and 8). Among the catalysts, CuO(30)$MgAlO_y$ demonstrates the highest yield of monoaromatic compounds of 9.7 wt.% compared with the others. Due to its relatively high yield of monoaromatic compounds among the catalysts, CuO(30)$MgAlO_y$ is considered as an appropriate catalyst to find

optimum reaction conditions such as temperature and time for lignin depolymerization.

In order to find the optimum reaction temperature for depolymerization of lignin, the reaction was performed at 360 °C, 400 °C, 440 °C and 480 °C for 4 h and the results are displayed in the Table 4-1 (Entry 2, 3, 4 and 7). With increasing the reaction temperature, the yield of monoaromatic compounds increases significantly (from 4.7 wt.% to 42.1 wt.%). According to the result, the optimum reaction temperature can be regarded as 480 °C where, however, the temperature region is categorized as pyrolysis [22]. Since current research is focused on solvolysis region (supercritical ethanol), so pyrolysis region should be excluded. In this respect, the optimum reaction temperature is selected as 440 °C. Meanwhile, Fang *et al*. has stated that the degree of depolymerization of lignin can be determined by the oil yield which consists of such as monomeric phenols, higher molecular phenols and aromatic hydrocarbons [97]. The results described in current work demonstrate that the yield of monoaromatic compounds is clearly affected by the reaction temperature, indicating that the degree of depolymerization of lignin increases by increasing the reaction temperature up to 440 °C.

Then, lignin depolymerization reaction was conducted at 440 °C over CuO(30)$MgAlO_y$ by varying time (4 h, 5 h and 6 h) to find the optimum reaction

time. As described in Table 4-1 (Entry 4, 5 and 6), the yield of monoaromatic compounds shows a volcano shape with respect to the reaction time; the maximum yield of monoaromatic compounds is 23.9 wt.% after reaction for 5 h. In summary, the optimum reaction conditions are selected as 440 ^{o}C for 5 h.

Table 4-1. Yield of monoaromatic compounds over the catalysts

Entry	Catalyst	Reaction temp. (^{o}C)	Reaction time (h)	Yield of monoaromatic compounds (wt.%)
1	10 wt.% Ni/C	400	4	4.8
2	$CuO(30)MgAlO_y$	360	4	4.7
3		400	4	9.7
4		440	4	21.1
5			5	23.9
6			6	22.6
7		480 (Pyrolysis)	4	42.1
8	10 wt.% Ni/ZSM-5(200)	400	4	4.6
9	None	440	5	5.0
10	10 wt.% Ni/ZSM-5(200)			12.5
11	10 wt.% Co/ZSM-5(200)			14.8
12	5 wt.% Cu/ZSM-5(200)			11.3
13	30 wt.% Cu/ZSM-5(200)			10.8
14	ZSM-5(30)			89.4
15	10 wt.% Cu/ZSM-5(30)			98.2
16	10 wt.% Cu/ZSM-5(50)			84.9
17	10 wt.% Cu/ZSM-5(80)			39.5
18	10 wt.% Cu/ZSM-5(200)			15.3

4.3.2 ZSM-5-supported catalysts for lignin depolymerization

Lignin depolymerization reaction was performed over both without catalyst (blank reaction) and ZSM-5 supported catalysts in supercritical ethanol at 440 ^{o}C for 5 h. Table 4-1 exhibits the yield of monoaromatic compounds quantified by using GC-FID. In case of the blank reaction, the yield of monoaromatic compounds is 5.0 wt.% (Entry 9). Meanwhile, the yield of monoaromatic compounds over ZSM-5 supported catalysts is shown in Table 4-1 as well. At first, among various transition metals (Ni, Co and Cu) supported on ZSM-5(200), 10 wt.% Cu/ZSM-5(200) shows the highest yield (15.3 wt.%) of monoaromatic compounds. Because the optimum metal is considered as Cu, the loading of Cu onto the ZSM-5(200) is varied from 5 wt.% to 30 wt.%. (Table 4-1, Entry 12and 13). Consequently, the maximum yield of monoaromatic compounds is obtained by applying Cu/ZSM-5(200) with Cu loading of 10 wt.%. This result indicates that the presence of the catalyst clearly enhances monoaromatic yield.

Finally, the Si/Al_2 ratio of ZSM-5 was varied from 30 to 200, while the loading of Cu was fixed as 10 wt.%. By changing the Si/Al_2 ratio of ZSM-5, the yield of monoaromatic compounds drastically increases (Table 4-1, Entry 15-18). The highest yield of monoaromatic compounds is observed over 10 wt.% Cu/ZSM-5(30) as 98.2 wt.% among the catalysts. Besides ZSM-5(30)-

supported catalyst, 10 wt.% Cu/ZSM-5(50) and 10 wt.% Cu/ZSM(80) also exhibit the relatively high yield of monoaromatic compounds (84.9 wt.% and 39.5 wt.%, respectively). Therefore, in order to elucidate the result, in-depth analysis over the 10 wt.% Cu/ZSM-5 as a function of the Si/Al_2 ratio were performed.

Figure 4-1 displays the distributions of monoaromatic compounds identified and quantified by GC-MS and GC-FID analysis over the catalysts. Benzaldehyde, ethylbenzene, m-xylene and toluene are mainly produced from the depolymerization of Protobind lignin. By decreasing the Si/Al_2 ratio, the amount of monoaromatic compounds gradually increases, which is well related to the yield of monoaromatic compounds.

Meanwhile, HSQC NMR analysis was performed to observe the changes of raw lignin and THF-soluble lignin after the lignin depolymerization reaction. In the side-chain region (Figure 4-2(A)), methoxy ($-OCH_3$), β-O-4 linkage (A), β-β linkage (B) and β-5 linkage (C) are clearly observed in Protobind lignin. By ^{13}C-^{1}H correlation for α, β and γ positions, the presence of β-O-4 is identified. The ^{13}C-^{1}H correlation in resinol substructures is displayed for β-β and that in phenylcoumarane substructures is shown for β-5. In addition, ρ-hydroxylcinnamyl alcohol end-groups (I) and β-D-xylopyranoside are also observed. The observation of the latter implies the formation or the presence of

furan compounds [50, 66]. Meanwhile, in the aromatic region (Figure 4- 2(B)), etherified syringyl units (S), oxidized (Cα =O) syringyl units (S'), guaiacyl units (G), ferulate (FA), ρ-hydroxyphenyl units (H) and ρ-coumarate (ρCA) are observed in raw Protobind lignin. This result is consistent with the previous report [66, 98].

After lignin depolymerization reaction, all the signals observed in the aromatic region completely disappear in the THF-soluble lignin over 10 wt.% Cu/ZSM-5(30) catalysts (not shown). It indicates that during the reaction, S, S'. G, FA, H and ρCA units in Protobind lignin are decomposed, resulting in the production of monoaromatic compounds. Meanwhile, in the side-chain region, a few signals are observed in the THF-soluble lignin over 10wt.% Cu/ZSM-5(30) (Figure 4-3). The methoxy signal is observed in the catalyst and the intensity of the signal decreases significantly compared with raw Protobind lignin (Figure 4-2(A)). The decrement of the signal corresponding to methoxy means that the hydrogenolysis reaction occurs over the catalysts, which is consistent with previous work [66, 99].

The products containing ethyl groups are also identified by HSQC NMR as evidenced by the signal concerning ethylated products marked with an asterisk (*) in Figure 4-3. This result means that ethylation between monoaromatic compounds and ethanol occurs during the reaction. Indeed, ethylated products

such as 2-ethylphenol, o-cresol and ethylbenzene are also detected by GC in the liquid product.

Meanwhile, in order to confirm the role of Cu, lignin depolymerization was conducted in the same condition by using Cu-free catalyst, ZSM-5(30). As a result, the yield of monoaromatic compounds is 89.4 wt.% (Table 4-1, Entry 14), which is lower than that of 10 wt.% Cu/ZSM-5(30). Based on the result, it can be speculated that the presence of Cu metals may play a certain role in enhancing the lignin depolymerization.

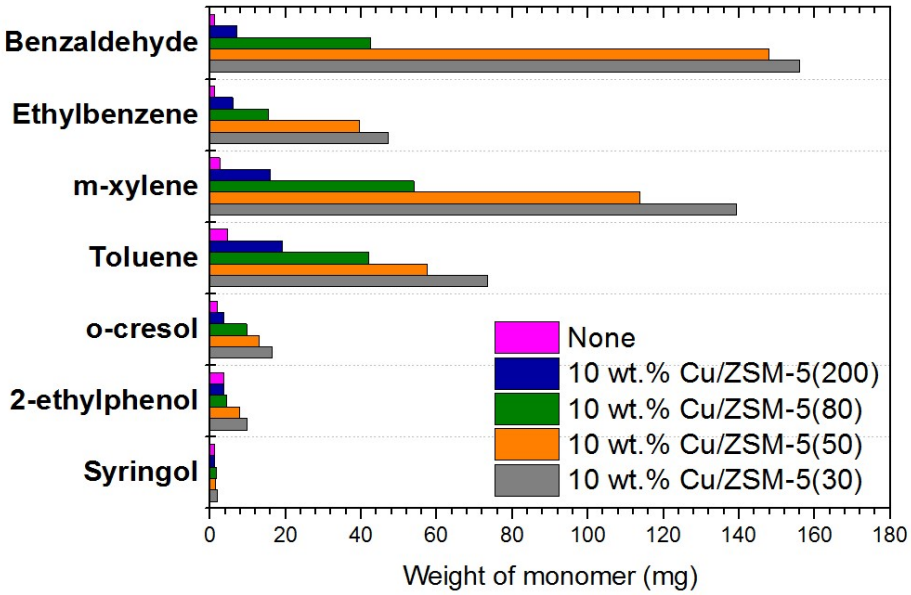

Figure 4-1. Distributions of selected monoaromatic compounds over the catalysts at 440 °C for 5 h.

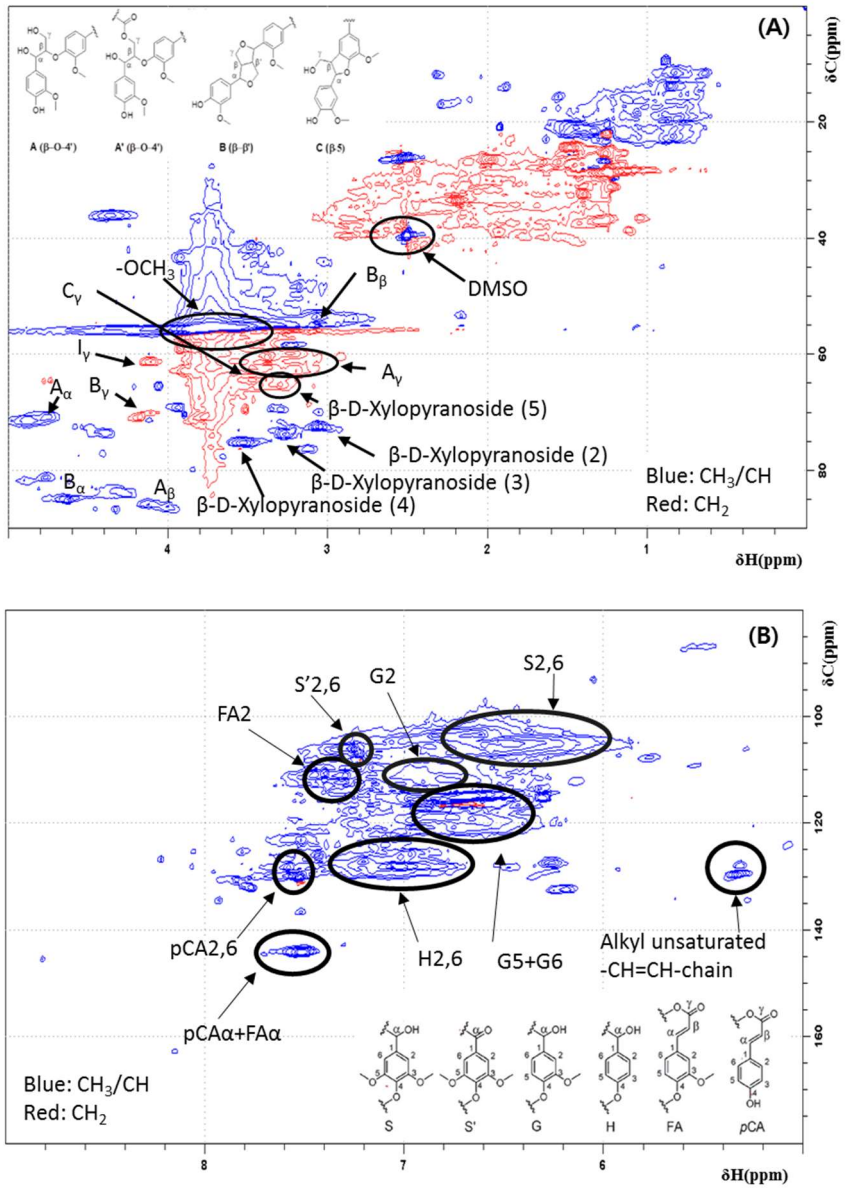

Figure 4-2. HSQC NMR spectra of Protobind lignin: (A) the side-chain region (B) the aromatic region.

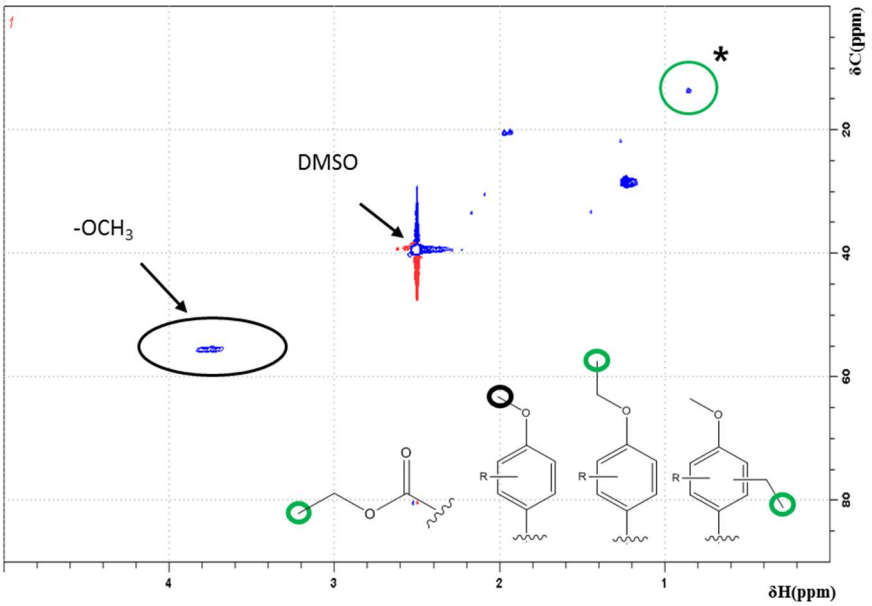

Figure 4-3. The side-chain region of HSQC NMR spectra of THF-soluble lignin after the reaction by using 10 wt.% Cu/ZSM-5(30) at 440 °C for 5 h.

4.3.3 Physical properties of 10 wt.% Cu/ZSM-5(ratio) catalysts

As shown in Table 4-2, the difference in the amount of the Cu loading between the experimental value and the theoretical value exists. However, the experimental values over the Cu loading among the samples are almost identical from 7.26 % to 7.54 %. Meanwhile, the experimental values of the Si/Al_2 ratio of ZSM-5 is slightly larger than the theoretical values. All catalysts have almost similar BET surface area between 331 m^2/g to 365 m^2/g, expect for 10 wt.% Cu/ZSM-5(80), which has the largest BET surface area as 426 m^2/g. However, the BET surface area is not related to the catalytic activity. Meanwhile, by increasing the Si/Al_2 ratio of ZSM-5, the external surface area increases from 98 m^2/g to 237 m^2/g. In the results of XRD analysis (Figure 4-4), the patterns of XRD assigned to ZSM-5 are displayed in all catalysts, indicating that even after Cu loading, the structure of ZSM-5 is well maintained. In addition, the patterns of XRD corresponding to Cu metal (43 ^{o} and 51 ^{o}) are also observed in all catalysts. The crystallinity of Cu metal over the catalysts is almost identical since the peak intensity of Cu metal phase at 43 ^{o} is also similar (the error range is about ± 10 %). In order to understand the morphology of the catalysts, SEM analysis was conducted and the SEM micrographs show in Figure 4-5. By varying the Si/Al_2 ratio of ZSM-5, the morphology of the catalysts is remarkably changed. As the Si/Al_2 ratio is the low such as 30 and

50, the particles demonstrate nearly cubic and/or schistose morphology (irregular morphology) with the particle size of about 200 nm, whereas the Si/Al_2 ratio is getting high such as 80 and 200, the particles have spherical morphology with the size of > 1 μm. Based on the result, it can be claimed that the morphology and the particle size of the catalysts are considerably different by changing the Si/Al_2 ratio in Cu/ZSM-5 [100].

Table 4-2. Results of ICP-AES and N_2 physisorption of the ZSM-5(ratio)-supported catalysts

Entry	Catalyst	ICP-MS		N_2 physisorption	
		Cu (%)	Si/Al_2	S_{BET} (m^2/g)	$S_{external}$ (m^2/g)
1	10 wt.% Cu/ZSM-5(30)	7.54	34	311	98
2	10 wt.% Cu/ZSM-5(50)	7.44	60	365	135
3	10 wt.% Cu/ZSM-5(80)	7.45	84	426	141
4	10 wt.% Cu/ZSM-5(200)	7.26	227	355	237

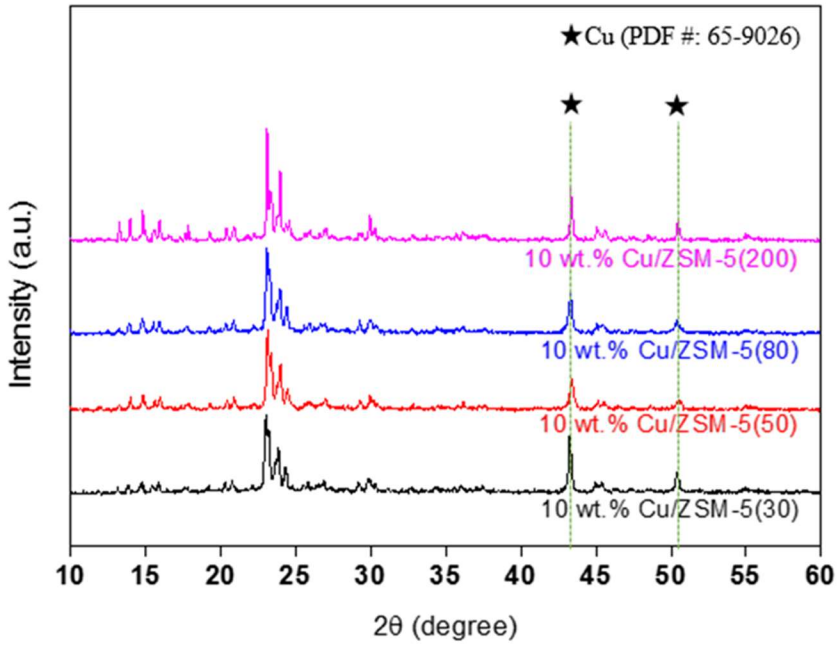

Figure 4-4. The XRD patterns of as-reduced 10 wt.% Cu/ZSM-5(ratio) catalysts; ratio of 30, 50, 80 and 200.

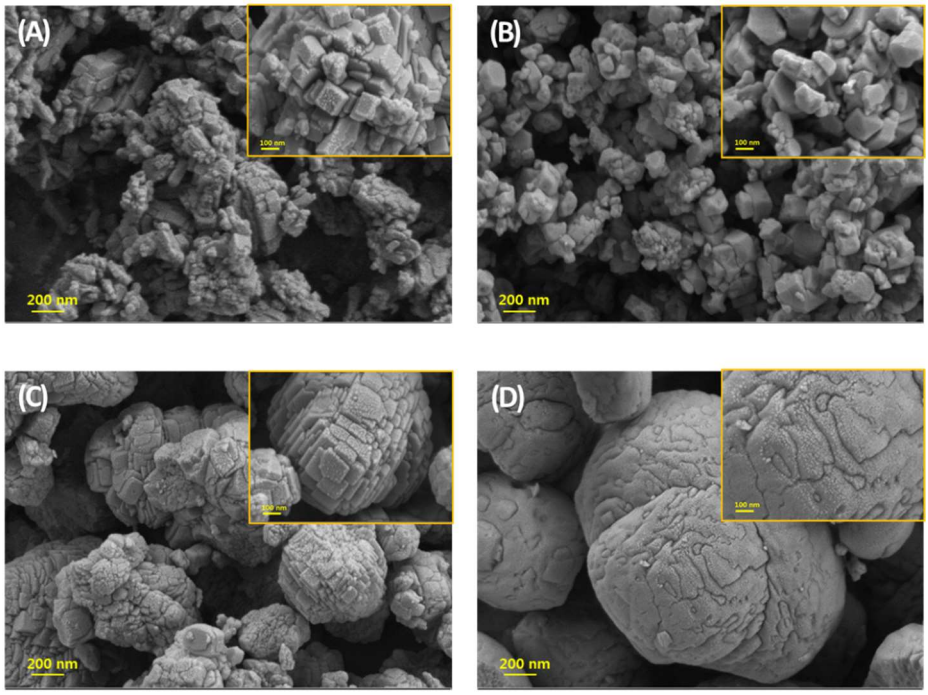

Figure 4-5. SEM images of as-reduced 10 wt.% Cu/ZSM-5 with (A) Si/Al_2(30), (B) Si/Al_2(50), (C) Si/Al_2(80) and (D) Si/Al_2(200).

4.3.4 Acidic properties of 10 wt.% Cu/ZSM-5(ratio) catalysts

In order to investigate the acidic properties of the catalysts, NH_3-TPD was conducted and the spectra are displayed in Figure 4-6. Two main desorption peaks are observed in the catalysts. The first peak below 350 ^oC is attributed to the weak acid sites of the catalysts, while the second peak above 350 ^oC originates from the strong acid sites [101, 102]. The amount of acid sites in the high temperature region is determined, which is normalized by external surface area since lignin is expected to access only to the external surface of Cu/ZSM-5 (Table 4-3). The acid density ($mmol/m^2$) of the catalysts increases by decreasing the Si/Al_2 ratio from 200 to 30; the order is followed by 10 wt.% Cu/ZSM-5(30): 3.2 $mmol/m^2$ > 10 wt.% Cu/ZSM-5 (50): 2.5 $mmol/m^2$ > 10 wt.% Cu/ZSM-5(80): 1.8 $mmol/m^2$ > 10 wt.% Cu/ZSM-5(200): 0.6 $mmol/m^2$. According to the previous research, the acidity increases with decreasing the Si/Al_2 ratio due to the increment of not only extra-framework aluminum content but also in the framework [103]. It was found that our result was consistent with previous work.

Figure 4-7 demonstrates the relationship between yield of monoaromatic compounds and acid density of 10 wt.% Cu/ZSM-5 as a function of the Si/Al_2 ratio catalysts. The yield of monoaromatic compounds and the acid density data were taken from Table 4-1 and 4-3, respectively. The yield of monoaromatic

compounds increases with increasing the acid density of the catalysts. Among the catalysts, 10 wt.% Cu/ZSM-5(30) shows the highest acid density (3.2 mmol/m^2), resulting in the highest yield of monoaromatic compounds. It can be concluded that the acid density of Cu/ZSM-5 plays a crucial role in depolymerization lignin in supercritical ethanol.

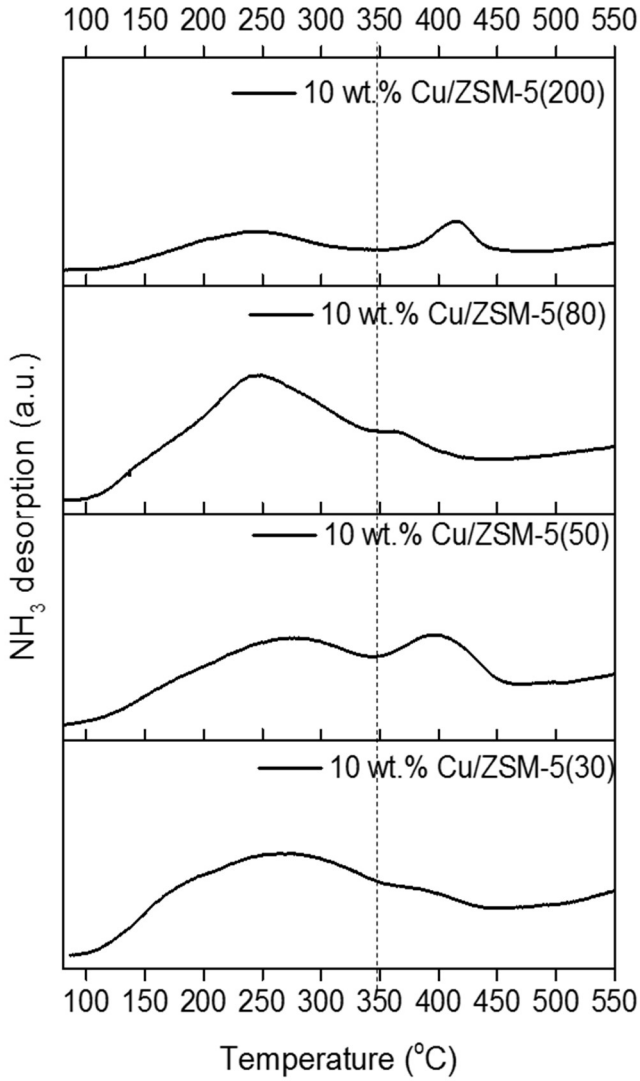

Figure 4-6. NH_3-TPD spectra of as-reduced 10 wt.% Cu/ZSM-5(ratio) catalysts.

Table 4-3. Quantity of acid sites at high temperature of the catalysts

Entry	Catalyst	Acid density ($mmol/m^2$)
1	10 wt.% Cu/ZSM-5(30)	3.2
2	10 wt.% Cu/ZSM-5(50)	2.5
3	10 wt.% Cu/ZSM-5(80)	1.8
4	10 wt.% Cu/ZSM-5(200)	0.6

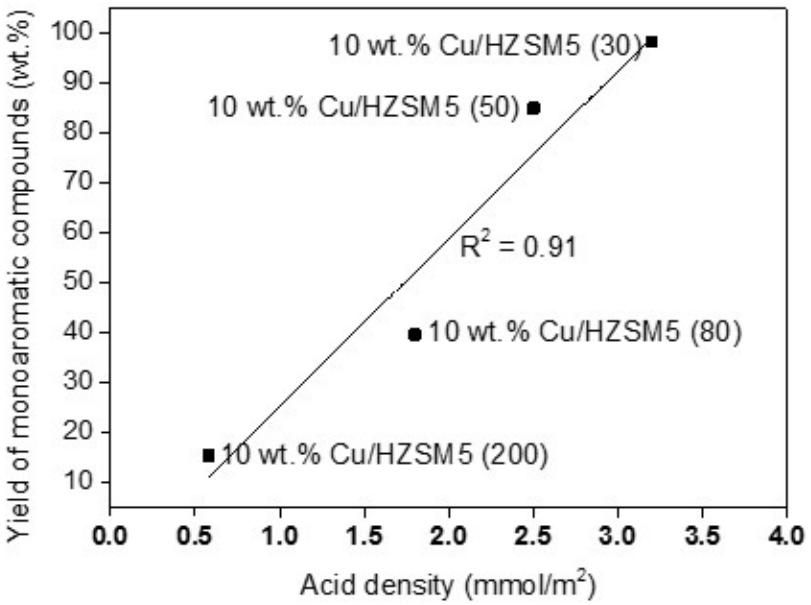

Figure 4-7. Relationship between the yield of monoaromatic compounds and the acid density of the catalysts.

5. Summary and Conclusions

The Al_2O_3-supported catalysts and the carbon-supported catalysts were applied for decomposition of BPE and the results of the yield of phenol and toluene were compared. It was confirmed that the carbon-supported catalysts were more suitable for decomposition of BPE compared to Al_2O_3-supported catalysts. In addition, Ru catalysts were the most reactive for decomposition of BPE because these catalysts were highly dispersed with small particles (about

1.5 nm) among the various metal catalysts supported on carbon. Meanwhile, the amount of generated H_2 was the most over 5 wt.% Pt/C among the three different metal catalysts (Ru, Pt and Ni), which was consistent with the previous report. It is found that 5 wt.% Pt/C in supercritical ethanol catalyzes alkylation, leading to the production of alkylated phenols.

We investigated the depolymerization of concentrated sulfuric acid hydrolysis lignin (CSAHL) over MO(X)$MgAlO_y$ catalysts (M = Cu, Ni or Co) in supercritical ethanol without additional hydrogen supply to acquire high monoaromatic yield. According to our results, Cu was selected as the optimum metal among Co, Ni and Cu with the highest yield of monoaromatic compounds of 18.4 wt.% when incorporated into $MgAlO_y$. When it comes to the amount of Cu loading, the optimum Cu loading was 30 wt.%, which showed the highest the number of acid sites. Meanwhile, we found that as the Cu loading exceeded 40 wt.%, there had been the decline of acid sites and the remarkable sintering of Cu metal during reaction, resulting in the decrement of monoaromatic yield.

The lignin depolymerization of Protobind lignin (PL) was performed over various parameters (catalysts, temperature and time) in supercritical ethanol without supplying extra hydrogen. Based on the result, the optimum reaction conditions (temperature and time) were selected as 440 ºC and 5 h. With the reaction conditions, ZSM-5-supported catalysts were applied to get the high

yield of monoaromatic compounds from the depolymerization of Protobind lignin. Therefore, various variables such as the types of transition metals (Co, Ni and Cu), the amount of metal loading (5 wt.%, 10 wt. % and 30 wt.% of Cu) and the Si/Al_2 ratio (30, 50, 80 and 200) were explored for lignin depolymerization at 440 ^oC for 5 h in supercritical ethanol. As a result, 10 wt.% Cu/ZSM-5(30) showed the highest yield of monoaromatic compounds as 98.2 wt.%. In addition, the linear correlation between yield of monoaromatic compounds and the acid density of Cu/ZSM-5 with various the Si/Al_2 ratios was obtained. It can be explained by the fact that with decreasing the Si/Al_2 ratio, the aluminum content of extra-framework increased, leading to the increment of the acidity of the catalyst. Consequently, the yield of monoaromatic compounds increased. It was also found that the presence of Cu on the ZSM-5 enhanced the lignin depolymerization.

Bibliography

[1] A. Demirbaş, Biomass resource facilities and biomass conversi on processing for fuels and chemicals, Energ Convers Manage, 42 (2001) 1357-1378.

[2] A. Demirbas, Biorefineries: Current activities and future devel opments, Energ Convers Manage, 50 (2009) 2782-2801.

[3] D.Y. Rachel-Tang, A. Islam, Y.H. Taufiq-Yap, Bio-oil product ion via catalytic solvolysis of biomass, Rsc Adv, 7 (2017) 7820-7 830.

[4] R. Singh, A. Prakash, S.K. Dhiman, B. Balagurumurthy, A.K. Arora, S.K. Puri, T. Bhaskar, Hydrothermal conversion of lignin t o substituted phenols and aromatic ethers, Bioresource Technol, 1 65 (2014) 319-322.

[5] F. Yan, R. Ma, X. Ma, K. Cui, K. Wu, M. Chen, Y. Li, Eth anolysis of Kraft lignin to platform chemicals on a MoC1-x/Cu-M gAlOz catalyst, Applied Catalysis B: Environmental, 202 (2017) 3 05-313.

[6] R. Rajappagowda, A.M. Numan-Al-Mobin, B. Yao, R.D. Coo k, A. Smirnova, Toward Selective Lignin Liquefaction: Synergistic Effect of Hetero- and Homogeneous Catalysis in Sub- and Super critical Fluids, Energ Fuel, 31 (2017) 578-586.

[7] J. Zakzeski, P.C.A. Bruijnincx, A.L. Jongerius, B.M. Weckhuy sen, The Catalytic Valorization of Lignin for the Production of R enewable Chemicals, Chemical Reviews, 110 (2010) 3552-3599.

[8] I. Klein, C. Marcum, H. Kenttamaa, M.M. Abu-Omar, Mecha nistic investigation of the Zn/Pd/C catalyzed cleavage and hydrode oxygenation of lignin, Green Chem, 18 (2016) 2399-2405.

[9] Y. Chen, F. Wang, Y. Jia, N. Yang, X. Zhang, One-step etha nolysis of lignin into small-molecular aromatic hydrocarbons over

nano-SiC catalyst, Bioresource Technol, 226 (2017) 145-149.
[10] P. Azadi, O.R. Inderwildi, R. Farnood, D.A. King, Liquid fu els, hydrogen and chemicals from lignin: A critical review, Rene wable and Sustainable Energy Reviews, 21 (2013) 506-523.
[11] R. Beauchet, F. Monteil-Rivera, J.M. Lavoie, Conversion of l ignin to aromatic-based chemicals (L-chems) and biofuels (L-fuel s), Bioresource Technol, 121 (2012) 328-334.
[12] M.M. Hossain, L. Aldous, Ionic Liquids for Lignin Processin g: Dissolution, Isolation, and Conversion, Australian Journal of Ch emistry, 65 (2012) 1465-1477.
[13] M. Saisu, T. Sato, M. Watanabe, T. Adschiri, K. Arai, Conv ersion of Lignin with Supercritical Water−Phenol Mixtures, Energ Fuel, 17 (2003) 922-928.
[14] E. Dorrestijn, L.J.J. Laarhoven, I.W.C.E. Arends, P. Mulder, The occurrence and reactivity of phenoxyl linkages in lignin and low rank coal, Journal of Analytical and Applied Pyrolysis, 54 (2 000) 153-192.
[15] M.P. Pandey, C.S. Kim, Lignin Depolymerization and Conve rsion: A Review of Thermochemical Methods, Chem Eng Technol, 34 (2011) 29-41.
[16] R.J.A. Gosselink, E. de Jong, B. Guran, A. Abächerli, Co-or dination network for lignin—standardisation, production and applic ations adapted to market requirements (EUROLIGNIN), Industrial Crops and Products, 20 (2004) 121-129.
[17] Z. Strassberger, A.H. Alberts, M.J. Louwerse, S. Tanase, G. Rothenberg, Catalytic cleavage of lignin [small beta]-O-4 link mi mics using copper on alumina and magnesia-alumina, Green Che m, 15 (2013) 768-774.
[18] N. Yan, C. Zhao, P.J. Dyson, C. Wang, L.-t. Liu, Y. Kou, Selective Degradation of Wood Lignin over Noble-Metal Catalysts

in a Two-Step Process, Chemsuschem, 1 (2008) 626-629.
[19] M.A. Jackson, D.L. Compton, A.A. Boateng, Screening heter ogeneous catalysts for the pyrolysis of lignin, Journal of Analytic al and Applied Pyrolysis, 85 (2009) 226-230.
[20] G.S. Macala, T.D. Matson, C.L. Johnson, R.S. Lewis, A.V. I retskii, P.C. Ford, Hydrogen Transfer from Supercritical Methanol over a Solid Base Catalyst: A Model for Lignin Depolymerization, Chemsuschem, 2 (2009) 215-217.
[21] K.B.H. Finch, R.M. Richards, A. Richel, A.V. Medvedovici, N.G. Gheorghe, M. Verziu, S.M. Coman, V.I. Parvulescu, Catalyti c hydroprocessing of lignin under thermal and ultrasound conditio ns, Catalysis Today, 196 (2012) 3-10.
[22] B. Joffres, D. Laurenti, N. Charon, A. Daudin, A. Quignard, C. Geantet, Thermochemical Conversion of Lignin for Fuels and Chemicals: A Review, Oil & Gas Science and Technology-Revue D Ifp Energies Nouvelles, 68 (2013) 753-763.
[23] R.J.A. Gosselink, W. Teunissen, J.E.G. van Dam, E. de Jong, G. Gellerstedt, E.L. Scott, J.P.M. Sanders, Lignin depolymerisatio n in supercritical carbon dioxide/acetone/water fluid for the produ ction of aromatic chemicals, Bioresource Technol, 106 (2012) 173 -177.
[24] T. Aysu, M.M. Küçük, Liquefaction of giant fennel (Ferula orientalis L.) in supercritical organic solvents: Effects of liquefacti on parameters on product yields and character, The Journal of Su percritical Fluids, 83 (2013) 104-123.
[25] A.P.S. Chouhan, A.K. Sarma, Modern heterogeneous catalysts for biodiesel production: A comprehensive review, Renewable an d Sustainable Energy Reviews, 15 (2011) 4378-4399.
[26] T. Nakagawa, H. Ozaki, T. Kamitanaka, H. Takagi, T. Mats uda, T. Kitamura, T. Harada, Reactions of supercritical alcohols

with unsaturated hydrocarbons, The Journal of Supercritical Fluids, 27 (2003) 255-261.
[27] C. Xu, T. Etcheverry, Hydro-liquefaction of woody biomass in sub- and super-critical ethanol with iron-based catalysts, Fuel, 87 (2008) 335-345.
[28] Z. Tang, Y. Zhang, Q. Guo, Catalytic Hydrocracking of Pyr olytic Lignin to Liquid Fuel in Supercritical Ethanol, Ind. Eng. C hem. Res., 49 (2010) 2040-2046.
[29] S. Brand, R.F. Susanti, S.K. Kim, H.-s. Lee, J. Kim, B.-I. S ang, Supercritical ethanol as an enhanced medium for lignocellulo sic biomass liquefaction: Influence of physical process parameters, Energy, 59 (2013) 173-182.
[30] D.S. Ross, J.E. Blessing, Alcohols as H-donor media in coal conversion. 1. Base-promoted H-donation to coal by isopropyl alc ohol, Fuel, 58 (1979) 433-437.
[31] F. Cavani, F. Trifirò, A. Vaccari, Hydrotalcite-type anionic c lays: Preparation, properties and applications, Catalysis Today, 11 (1991) 173-301.
[32] A. Vaccari, Preparation and catalytic properties of cationic a nd anionic clays, Catalysis Today, 41 (1998) 53-71.
[33] X. Huang, C. Atay, T.I. Korányi, M.D. Boot, E.J.M. Hensen, Role of Cu–Mg–Al Mixed Oxide Catalysts in Lignin Depolymeri zation in Supercritical Ethanol, ACS Catal., 5 (2015) 7359-7370.
[34] G. Warner, T.S. Hansen, A. Riisager, E.S. Beach, K. Barta, P.T. Anastas, Depolymerization of organosolv lignin using doped porous metal oxides in supercritical methanol, Bioresource Techno l, 161 (2014) 78-83.
[35] T.D. Matson, K. Barta, A.V. Iretskii, P.C. Ford, One-Pot Cat alytic Conversion of Cellulose and of Woody Biomass Solids to Liquid Fuels, J Am Chem Soc, 133 (2011) 14090-14097.

[36] N.M. Al-Otaibi, G. Hutchings, Aromatization of Isobutene Us ing H-ZSM-5/Oxide Composite Catalysts, Catalysis Letters, 134 (2 010) 191-195.
[37] A.J. Foster, J. Jae, Y.-T. Cheng, G.W. Huber, R.F. Lobo, O ptimizing the aromatic yield and distribution from catalytic fast p yrolysis of biomass over ZSM-5, Applied Catalysis A: General, 4 23–424 (2012) 154-161.
[38] A. Veses, B. Puértolas, J.M. López, M.S. Callén, B. Solsona, T. García, Promoting Deoxygenation of Bio-Oil by Metal-Loaded Hierarchical ZSM-5 Zeolites, ACS Sustainable Chemistry & Engi neering, 4 (2016) 1653-1660.
[39] S.K. Singh, J.D. Ekhe, Solvent effect on HZSM-5 catalyzed solvolytic depolymerization of industrial waste lignin to phenols: s uperiority of the water-methanol system over methanol, Rsc Adv, 4 (2014) 53220-53228.
[40] J. Milovanović, N. Rajić, A.A. Romero, H. Li, K. Shih, R. Tschentscher, R. Luque, Insights into the Microwave-Assisted Mil d Deconstruction of Lignin Feedstocks Using NiO-Containing ZS M-5 Zeolites, ACS Sustainable Chemistry & Engineering, 4 (2016) 4305-4313.
[41] J. Zakzeski, A.L. Jongerius, P.C.A. Bruijnincx, B.M. Weckhu ysen, Catalytic Lignin Valorization Process for the Production of Aromatic Chemicals and Hydrogen, Chemsuschem, 5 (2012) 1602-1609.
[42] A.L. Jongerius, P.C.A. Bruijnincx, B.M. Weckhuysen, Liquid-phase reforming and hydrodeoxygenation as a two-step route to ar omatics from lignin, Green Chem, 15 (2013) 3049-3056.
[43] K. Barta, T.D. Matson, M.L. Fettig, S.L. Scott, A.V. Iretskii, P.C. Ford, Catalytic disassembly of an organosolv lignin via hyd rogen transfer from supercritical methanol, Green Chem, 12 (2010)

1640-1647.
[44] H. Prajitno, R. Insyani, J. Park, C. Ryu, J. Kim, Non-catalyt ic upgrading of fast pyrolysis bio-oil in supercritical ethanol and combustion behavior of the upgraded oil, Applied Energy, 172 (2 016) 12-22.
[45] C. Løhre, T. Barth, M. Kleinert, The effect of solvent and i nput material pretreatment on product yield and composition of bi o-oils from lignin solvolysis, Journal of Analytical and Applied P yrolysis, 119 (2016) 208-216.
[46] G.T. Neumann, B.R. Pimentel, D.J. Rensel, J.C. Hicks, Corre lating lignin structure to aromatic products in the catalytic fast py rolysis of lignin model compounds containing [small beta]-O-4 lin kages, Catal Sci Technol, 4 (2014) 3953-3963.
[47] K. Barta, G.R. Warner, E.S. Beach, P.T. Anastas, Depolymer ization of organosolv lignin to aromatic compounds over Cu-dope d porous metal oxides, Green Chem, 16 (2014) 191-196.
[48] B. Güvenatam, E.H.J. Heeres, E.A. Pidko, E.J.M. Hensen, Le wis-acid catalyzed depolymerization of Protobind lignin in supercri tical water and ethanol, Catalysis Today, 259, Part 2 (2016) 460-466.
[49] M. Zabeti, W.M.A. Wan Daud, M.K. Aroua, Activity of soli d catalysts for biodiesel production: A review, Fuel Processing Te chnology, 90 (2009) 770-777.
[50] M. Kim, D. Son, J.-W. Choi, J. Jae, D.J. Suh, J.-M. Ha, K. -Y. Lee, Production of phenolic hydrocarbons using catalytic depo lymerization of empty fruit bunch (EFB)-derived organosolv lignin on Hβ-supported Ru, Chemical Engineering Journal, 309 (2017) 187-196.
[51] S. De, A.M. Balu, J.C. van der Waal, R. Luque, Biomass-Der ived Porous Carbon Materials: Synthesis and Catalytic Application

s, Chemcatchem, 7 (2015) 1608-1629.
[52] M. Toda, A. Takagaki, M. Okamura, J.N. Kondo, S. Hayash i, K. Domen, M. Hara, Green chemistry: Biodiesel made with sug ar catalyst, Nature, 438 (2005) 178-178.
[53] E. Lam, J.H.T. Luong, Carbon Materials as Catalyst Support s and Catalysts in the Transformation of Biomass to Fuels and C hemicals, ACS Catal., 4 (2014) 3393-3410.
[54] J.K. Kim, J.K. Lee, K.H. Kang, J.W. Lee, I.K. Song, Cataly tic decomposition of phenethyl phenyl ether to aromatics over Pd –Fe bimetallic catalysts supported on ordered mesoporous carbon, Journal of Molecular Catalysis A: Chemical, 410 (2015) 184-192.
[55] I. Klein, B. Saha, M.M. Abu-Omar, Lignin depolymerization over Ni/C catalyst in methanol, a continuation: effect of substrate and catalyst loading, Catal Sci Technol, 5 (2015) 3242-3245.
[56] Q. Song, F. Wang, J. Xu, Hydrogenolysis of lignosulfonate i nto phenols over heterogeneous nickel catalysts, Chem Commun, 48 (2012) 7019-7021.
[57] R.H. Schlosberg, W.H. Davis, T.R. Ashe, Pyrolysis studies o f organic oxygenates. 2. Benzyl phenyl ether pyrolysis under batc h autoclave conditions, Fuel, 60 (1981) 201-204.
[58] J. He, C. Zhao, J.A. Lercher, Ni-catalyzed cleavage of aryl ethers in the aqueous phase, J Am Chem Soc, 134 (2012) 20768-20775.
[59] B.C. Wu, M.T. Klein, S.I. Sandler, Influence of supercritical fluid solvent density on benzyl phenyl ether pyrolysis: indications of diffusional limitations, Energ Fuel, 5 (1991) 453-458.
[60] B.C. Wu, M.T. Klein, S.I. Sandler, The Benzylphenylether th ermolysis mechanism: Insights from phase behavior, Aiche J, 36 (1990) 1129-1136.
[61] J.K. Kim, J.K. Lee, K.H. Kang, J.C. Song, I.K. Song, Select

ive cleavage of CO bond in benzyl phenyl ether to aromatics ove r Pd–Fe bimetallic catalyst supported on ordered mesoporous carb on, Applied Catalysis A: General, 498 (2015) 142-149.
[62] T. Sato, G. Sekiguchi, T. Adschiri, K. Arai, Non-catalytic an d selective alkylation of phenol with propan-2-ol in supercritical water, Chem Commun, (2001) 1566-1567.
[63] C.A. Fisk, T. Morgan, Y. Ji, M. Crocker, C. Crofcheck, S.A. Lewis, Bio-oil upgrading over platinum catalysts using in situ ge nerated hydrogen, Applied Catalysis A: General, 358 (2009) 150-1 56.
[64] V. Roberts, S. Fendt, A.A. Lemonidou, X. Li, J.A. Lercher, Influence of alkali carbonates on benzyl phenyl ether cleavage pat hways in superheated water, Applied Catalysis B: Environmental, 95 (2010) 71-77.
[65] K.Y. Nandiwale, N.D. Galande, S.A. Raut, V.V. Bokade, Be nzylation of acetic acid to benzyl acetate over highly active and r eusable Micro/Meso-HZSM-5, Chemical Engineering Research and Design, 93 (2015) 584-590.
[66] X.M. Huang, T.I. Koranyi, M.D. Boot, E.J.M. Hensen, Catal ytic Depolymerization of Lignin in Supercritical Ethanol, Chemsus chem, 7 (2014) 2276-2288.
[67] J.-Y. Kim, S. Oh, H. Hwang, T.-s. Cho, I.-G. Choi, J.W. C hoi, Effects of various reaction parameters on solvolytical depoly merization of lignin in sub- and supercritical ethanol, Chemospher e, 93 (2013) 1755-1764.
[68] Y. Guo, S.Z. Wang, D.H. Xu, Y.M. Gong, H.H. Ma, X.Y. Tang, Review of catalytic supercritical water gasification for hydr ogen production from biomass, Renewable and Sustainable Energy Reviews, 14 (2010) 334-343.
[69] Q. Song, F. Wang, J. Cai, Y. Wang, J. Zhang, W. Yu, J. X

u, Lignin depolymerization (LDP) in alcohol over nickel-based cat alysts via a fragmentation-hydrogenolysis process, Energ Environ Sci, 6 (2013) 994-1007.
[70] A. Pineda, A.F. Lee, Heterogeneously catalyzed lignin depoly merization, Applied Petrochemical Research, (2016) 1-14.
[71] M. Kleinert, T. Barth, Phenols from Lignin, Chem Eng Tech nol, 31 (2008) 736-745.
[72] W. Xu, S.J. Miller, P.K. Agrawal, C.W. Jones, Depolymeriza tion and Hydrodeoxygenation of Switchgrass Lignin with Formic Acid, Chemsuschem, 5 (2012) 667-675.
[73] S. Huang, N. Mahmood, M. Tymchyshyn, Z. Yuan, C. Xu, Reductive de-polymerization of kraft lignin for chemicals and fuel s using formic acid as an in-situ hydrogen source, Bioresource Te chnol, 171 (2014) 95-102.
[74] P.T. Patil, U. Armbruster, M. Richter, A. Martin, Heterogene ously Catalyzed Hydroprocessing of Organosolv Lignin in Sub- an d Supercritical Solvents, Energ Fuel, 25 (2011) 4713-4722.
[75] A. Riaz, C.S. Kim, Y. Kim, J. Kim, High-yield and high-cal orific bio-oil production from concentrated sulfuric acid hydrolysis lignin in supercritical ethanol, Fuel, 172 (2016) 238-247.
[76] M.A. Aramendia, Y. Aviles, J.A. Benitez, V. Borau, C. Jime nez, J.M. Marinas, J.R. Ruiz, F.J. Urbano, Comparative study of Mg Al and Mg Ga layered double hydroxides, Microporous and Mesoporous Materials, 29 (1999) 319-328.
[77] J. Kong, L. Jiang, Z. Huo, X. Xu, D.G. Evans, J. Song, M. He, Z. Li, Q. Wang, L. Yan, Influence of the preparation process on the performance of three hydrotalcite-based De-SOx catalysts, Catalysis Communications, 40 (2013) 59-62.
[78] W.T. Reichle, S.Y. Kang, D.S. Everhardt, THE NATURE O F THE THERMAL-DECOMPOSITION OF A CATALYTICALLY

ACTIVE ANIONIC CLAY MINERAL, Journal of Catalysis, 101 (1986) 352-359.
[79] H. Hu, S. Cai, H. Li, L. Huang, L. Shi, D. Zhang, In Situ DRIFTs Investigation of the Low-Temperature Reaction Mechanis m over Mn-Doped Co3O4 for the Selective Catalytic Reduction o f NOx with NH3, The Journal of Physical Chemistry C, 119 (20 15) 22924-22933.
[80] R.L. Manfro, T.P.M.D. Pires, N.F.P. Ribeiro, M.M.V.M. Sou za, Aqueous-phase reforming of glycerol using Ni-Cu catalysts pre pared from hydrotalcite-like precursors, Catal Sci Technol, 3 (201 3) 1278-1287.
[81] G. Fornasari, S. Gusi, F. Trifiro, A. Vaccari, Cobalt mixed s pinels as catalysts for the synthesis of hydrocarbons, Ind. Eng. C hem. Res., 26 (1987) 1500-1505.
[82] W. Wanmolee, P. Daorattanachai, N. Laosiripojana, Depolym erization of Organosolv Lignin to Valuable Chemicals over Homo geneous and Heterogeneous Acid Catalysts, Energy Procedia, 100 (2016) 173-177.
[83] A.R.C. Morais, A.M. da Costa Lopes, R. Bogel-Łukasik, Car bon Dioxide in Biomass Processing: Contributions to the Green B iorefinery Concept, Chemical Reviews, 115 (2014) 3-27.
[84] R. Chaudhary, P.L. Dhepe, Solid base catalyzed depolymeriz ation of lignin into low molecular weight products, Green Chem, 19 (2017) 778-788.
[85] S. Zhu, J. Guo, X. Wang, J. Wang, W. Fan, Alcoholysis: A Promising Technology for Conversion of Lignocellulose and Platfo rm Chemicals, Chemsuschem, n/a-n/a.
[86] T. Sato, M. Osada, M. Watanabe, M. Shirai, K. Arai, Gasifi cation of Alkylphenols with Supported Noble Metal Catalysts in Supercritical Water, Ind. Eng. Chem. Res., 42 (2003) 4277-4282.

[87] M.R. Sturgeon, M.H. O'Brien, P.N. Ciesielski, R. Katahira, J. S. Kruger, S.C. Chmely, J. Hamlin, K. Lawrence, G.B. Hunsinger, T.D. Foust, R.M. Baldwin, M.J. Biddy, G.T. Beckham, Lignin d epolymerisation by nickel supported layered-double hydroxide catal ysts, Green Chem, 16 (2014) 824-835.
[88] P. Chen, Q. Zhang, R. Shu, Y. Xu, L. Ma, T. Wang, Catal ytic depolymerization of the hydrolyzed lignin over mesoporous c atalysts, Bioresource Technol, 226 (2017) 125-131.
[89] J. Jae, G.A. Tompsett, A.J. Foster, K.D. Hammond, S.M. Au erbach, R.F. Lobo, G.W. Huber, Investigation into the shape selec tivity of zeolite catalysts for biomass conversion, Journal of Catal ysis, 279 (2011) 257-268.
[90] T.R. Carlson, T.P. Vispute, G.W. Huber, Green Gasoline by Catalytic Fast Pyrolysis of Solid Biomass Derived Compounds, C hemsuschem, 1 (2008) 397-400.
[91] R.O. Idem, S.P.R. Katikaneni, N.N. Bakhshi, Catalytic conve rsion of canola oil to fuels and chemicals: roles of catalyst acidit y, basicity and shape selectivity on product distribution, Fuel Proc essing Technology, 51 (1997) 101-125.
[92] S.K. Singh, J.D. Ekhe, Towards effective lignin conversion: HZSM-5 catalyzed one-pot solvolytic depolymerization/hydrodeoxy genation of lignin into value added compounds, Rsc Adv, 4 (201 4) 27971-27978.
[93] C.A. Mullen, P.C. Tarves, A.A. Boateng, Role of Potassium Exchange in Catalytic Pyrolysis of Biomass over ZSM-5: Formati on of Alkyl Phenols and Furans, ACS Sustainable Chemistry & E ngineering, 5 (2017) 2154-2162.
[94] S. Jeong, G.H. Jang, D.H. Kim, Decomposition of Lignin Us ing MO–MgAlOy Mixed Oxide Catalysts (M=Co, Ni and Cu) in Supercritical Ethanol, Topics in Catalysis, (2017) 1-7.

[95] C. Busetto, G. Del Piero, G. Manara, F. Trifirò, A. Vaccari, Catalysts for low-temperature methanol synthesis. Preparation of C u Zn Al mixed oxides via hydrotalcite-like precursors, Journal of Catalysis, 85 (1984) 260-266.
[96] D. O. Klenov, G. N. Kryukova, L. M. Plyasova, Localizatio n of copper atoms in the structure of the ZnO catalyst for metha nol synthesis, J Mater Chem, 8 (1998) 1665-1669.
[97] Z. Fang, T. Sato, R.L. Smith Jr, H. Inomata, K. Arai, J.A. Kozinski, Reaction chemistry and phase behavior of lignin in high -temperature and supercritical water, Bioresource Technol, 99 (200 8) 3424-3430.
[98] T.Q. Yuan, S.N. Sun, F. Xu, R.C. Sun, ISOLATION AND PHYSICO-CHEMICAL CHARACTERIZATION OF LIGNINS FR OM ULTRASOUND IRRADIATED FAST-GROWING POPLAR WOOD, Bioresources, 6 (2011) 414-433.
[99] X. Huang, T.I. Koranyi, M.D. Boot, E.J.M. Hensen, Ethanol as capping agent and formaldehyde scavenger for efficient depoly merization of lignin to aromatics, Green Chem, (2015).
[100] C.-J. Jia, Y. Liu, W. Schmidt, A.-H. Lu, F. Schüth, Small-sized HZSM-5 zeolite as highly active catalyst for gas phase deh ydration of glycerol to acrolein, Journal of Catalysis, 269 (2010) 71-79.
[101] D. Shen, N. Liu, C. Dong, R. Xiao, S. Gu, Catalytic solvo lysis of lignin with the modified HUSYs in formic acid assisted by microwave heating, Chemical Engineering Journal, 270 (2015) 641-647.
[102] S. Lai, D. Meng, W. Zhan, Y. Guo, Y. Guo, Z. Zhang, G. Lu, The promotional role of Ce in Cu/ZSM-5 and in situ surfac e reaction for selective catalytic reduction of NOx with NH3, Rsc

Adv, 5 (2015) 90235-90244.
[103] Y. Gao, B. Zheng, G. Wu, F. Ma, C. Liu, Effect of the Si /Al ratio on the performance of hierarchical ZSM-5 zeolites for methanol aromatization, Rsc Adv, 6 (2016) 83581-83588.

6. 국 문 초 록

화석연료는 수요가 증가함에 따라 빠르게 고갈되고 있으므로 새로운 대체 자원이 필요하다. 바이오매스는 지구상에서 가장 풍부한 재생 가능한 탄소자원이므로, 유망한 대체 원료 중 하나로 주목 받고 있다. 2세대 바이오매스인 리그노셀룰로오스는 1세대 바이오매스와 달리 식량자원으로 이용되지 않는다. 특히, 리그노셀룰로오스 바이오매스의 구성성분 중 하나인 리그닌은 다량의 방향족 화합물들로 이루어진 무정형 고분자이며 탄소-탄소 및 탄소-산소 결합으로 이루어져 있어 고부가가치 화합물로 이용할 수 있다. 리그닌은 β-O-4 (46 ~ 60 %), α-O-4 (6 ~8 %) 그리고 4-O-5 (3.5 ~ 6.5 %)와 같은 탄소-산소 결합들이 주를 이루며 β-β (7 %), β-5 (6 ~ 12 %), β-1 (4.5 ~11 %) 그리고 5-5 (2 ~3 %)와 같은 탄소-탄소 결합들이 매우 적은 양으로 구성되어 있다. 따라서, 선택적인 탄소-산소 결합의 분해기술은 리그닌을 고부가가치 화합물로 전환시키기 위한 가장 중요한 기술이다.

수 년간 리그닌 분해로부터 고부가가치 화합물의 수율을 높이기 위하여 열분해, 가스화분해, 촉매접촉분해, 가용매분해와 같은 다양한 열화학적 분해기술들이 이용되었다. 그러나 리그닌의 난분해성 구조로 인해 리그닌을 고부가가치 화합물로 전환하기에 어려움이 있었다. 최근 몇 년 동안 가용매분해가 많은 주목을 받고 있는데 그 이유는 생성물의 수율이 높을 뿐만 아니라 얻어지는 생성물의 성질 또한 우수하기 때문이다. 특히,

초임계 알코올 (에탄올)을 이용한 가용매분해의 경우, 탄소-산소 결합 분해에 필수적인 수소를 자가발생 시킬 수 있기 때문에 더욱 주목 받고 있다. 또한, 적절한 촉매를 이용하면 선택적인 탄소-산소 결합의 분해가 가능하기 때문에 리그닌 분해반응에서 촉매와 초임계 알코올을 동시에 이용하는 방법이 최근 관심을 받고 있다.

따라서, 본 연구에서는 앞서 설명한 초임계 알코올을 이용한 가용매 분해와 촉매분해의 장점을 결합한 초임계 유체-촉매 시스템을 이용하여 리그닌의 주요 결합 중 하나인 α-O-4를 포함하는 모델화합물의 분해반응 경로를 연구하였고 나아가 리그닌 (강산당화 리그닌, 프로토바인드 리그닌)을 단일 방향족 화합물로 분해하는 연구를 수행하였다.

첫 번째로 α-O-4를 포함하는 모델 화합물인 벤질 페닐 에테르를 이용하여 초임계 에탄올 조건에서 추가의 외부 수소 공급 없이 모델 화합물 분해반응을 진행하였다. 그 결과, 탄소 지지체 촉매들이 알루미나 지지체 촉매들보다 생성물 (페놀 및 톨루엔)의 수율이 약 2배 이상 높았다. 또한, 담지 된 금속 (Ru, Pt 그리고 Ni)에 대하여 촉매 활성을 비교한 결과, Ru 금속을 이용한 경우, 생성물 (페놀 및 톨루엔) 수율이 96.4 %로 가장 높았다. 이는 세 가지 금속 중 Ru이 카본 지지체에 가장 작은 입자 크기로 (약 1.5 nm) 고 분산된 형태로 존재하기 때문이다. 생성된 수소의 양은 5 wt.% Pt/C 촉매에서 가장 많았으며 알킬화 페놀의 양도 가장 많았다. 이를 통해 세 가지 금속 촉매 중 Pt 촉매가 초임계 에탄올 조건에서 알킬화를 가장

촉진시킨다는 것을 유추할 수 있었다. 이 결과를 근거로 초임계 에탄올에서의 벤질 페닐 에테르의 반응 경로를 제시하였다.

두 번째로 강산당화 리그닌을 이용하여 초임계 에탄올 조건에서 다양한 촉매들에 대해 리그닌 분해반응을 수행하였다. 우선적으로 Co, Ni 그리고 Cu가 각각 30 wt.%씩 공침된 $MgAlO_y$ 기반 촉매의 경우, $CuO(30)MgAlO_y$ 촉매의 단일 방향족 수율이 18.4 wt.%로 세 촉매 중 가장 높았고 가장 많은 산점을 보유하고 있는 것이 관찰되었다. 따라서, 촉매표면의 산점이 리그닌 분해반응 중 단일 방향족 생산에 중요한 역할을 결정 짓는 주요 인자라고 할 수 있다. 또한, Cu 담지량이 10 wt.%에서 40 wt.%까지 증가함에 따라 단일 방향족 수율은 화산형 그래프 개형을 보이며 Cu 담지량이 30 wt.% 일 때 단일 방향족 수율이 가장 높았다. 암모니아 승온탈착 실험 결과 최대 산점은 Cu 담지량이 30 wt.%일 때 나타났고, 이는 반응실험 결과와도 일치했다. Cu 담지량이 30 wt.% 이상이 되면 산점이 감소하고 그로 인해 단일 방향족 수율도 감소하였다.

마지막으로, 프로토바인드 리그닌의 분해반응은 초임계 에탄올 조건에서 진행되었으며 제올라이트 기반 촉매를 이용하여 전이금속 (Co, Ni 그리고 Cu)의 종류, Cu 금속의 담지량 (5 wt.%, 10 wt.% 그리고 30wt.%), 마지막으로 Si/Al_2의 비율 (30, 50, 80 그리고 200)과 같은 다양한 변수들에 대해 관찰하였다. 그 결과, 10 wt.% Cu/ZSM-5(30) 촉매가 98.2 wt.%로 가장 높은 단일 방향족 수율을 나타내었고 이는 가장 많은 산 밀도 (3.2

mmol/m^2)를 갖고 있기 때문이었다. 또한, 산 밀도가 증가함에 따라 단일 방향족 수율이 증가하여 둘 사이의 선형관계가 성립됨을 확인하였다. 이로써, 촉매표면의 산 밀도는 프로토바인드 리그닌 분해반응에서 단일 방향족 생산을 위한 결정적인 요소라고 할 수 있다. HSQC NMR 분석을 통해 프로토바인드 리그닌의 분해는 수소화 반응을 통해 진행되는 것을 유추할 수 있었다. 또한, HSQC NMR 스펙트럼에서 에틸화 생성물 관련 신호가 관찰되었다. 이는 생성물 중 에틸화 생성물이 존재함을 의미하며 실제 생성물 분석 결과와 일치했다. 또한, Cu 금속의 첨가가 리그닌 분해반응을 향상시키는 데 중요한 역할을 한다는 것을 발견했다.

주요어: 리그닌의 촉매적 분해반응, 초임계 에탄올, 자가발생 수소, 산점
학 번: 2013-30989